UNIVERSIDAD DE INVESTIGACIÓN DE TECNOLOGÍA EXPERIMENTAL YACHAY

Escuela de Ciencias Físicas y Nanotecnología

TÍTULO: Dualities by gravitational decoupling in 2+1 dimensional spacetimes with cosmological term

Trabajo de integración curricular presentado como requisito para la obtención del título de Físico

Autor:

Anthony Sebastian Ramos Cisneros

Tutor:

Ph. D. Ernesto Antonio Medina Dagger

Co-Tutor:

Ph. D. Ernesto José Contreras Herrada

Urcuquí, Marzo 2020

SECRETARÍA GENERAL
(Vicerrectorado Académico/Cancillería)
ESCUELA DE CIENCIAS FÍSICAS Y NANOTECNOLOGÍA
CARRERA DE FÍSICA
ACTA DE DEFENSA No. UITEY-PHY-2020-00002-AD

En la ciudad de San Miguel de Urcuquí, Provincia de Imbabura, a los 6 días del mes de marzo de 2020, a las 16:30 horas, en el Aula 1 de la Universidad de Investigación de Tecnología Experimental Yachay y ante el Tribunal Calificador, integrado por los docentes:

Presidente Tribunal de Defensa	Dr. RAMIREZ VELASQUEZ JOSE MANUEL , Ph.D.
Miembro No Tutor	Dra. ROJAS CELY CLARA INES , Ph.D.
Tutor	Dr. MEDINA DAGGER, ERNESTO ANTONIO, Ph.D.

Se presenta el(la) señor(ita) estudiante **RAMOS CISNEROS, ANTHONY SEBASTIAN**, con cédula de identidad No. **1725075483**, de la **ESCUELA DE CIENCIAS FÍSICAS Y NANOTECNOLOGÍA**, de la Carrera de **FÍSICA**, aprobada por el Consejo de Educación Superior (CES), mediante Resolución **RPC-SO-39-No.456-2014**, con el objeto de rendir la sustentación de su trabajo de titulación denominado: **Dualities by gravitational decoupling in 2+1 dimensional spacetimes with cosmological term**, previa a la obtención del título de **FÍSICO/A**.

El citado trabajo de titulación, fue debidamente aprobado por el(los) docente(s):

Tutor	Dr. MEDINA DAGGER, ERNESTO ANTONIO, Ph.D.

Y recibió las observaciones de los otros miembros del Tribunal Calificador, las mismas que han sido incorporadas por el(la) estudiante.

Previamente cumplidos los requisitos legales y reglamentarios, el trabajo de titulación fue sustentado por el(la) estudiante y examinado por los miembros del Tribunal Calificador. Escuchada la sustentación del trabajo de titulación, que integró la exposición de el(la) estudiante sobre el contenido de la misma y las preguntas formuladas por los miembros del Tribunal, se califica la sustentación del trabajo de titulación con las siguientes calificaciones:

Tipo	Docente	Calificación
Tutor	Dr. MEDINA DAGGER, ERNESTO ANTONIO, Ph.D.	10,0
Presidente Tribunal De Defensa	Dr. RAMIREZ VELASQUEZ JOSE MANUEL , Ph.D.	9,9
Miembro Tribunal De Defensa	Dra. ROJAS CELY CLARA INES , Ph.D.	9,9

Lo que da un promedio de: **9.9 (Nueve punto Nueve)**, sobre 10 (diez), equivalente a: **APROBADO**

Para constancia de lo actuado, firman los miembros del Tribunal Calificador, el/la estudiante y el/la secretario ad-hoc.

RAMOS CISNEROS, ANTHONY SEBASTIAN
Estudiante

Dr. RAMIREZ VELASQUEZ JOSE MANUEL , Ph.D.
Presidente Tribunal de Defensa

Firmado electrónicamente por:
JOSE MANUEL
RAMIREZ
VELASQUEZ

Dr. MEDINA DAGGER, ERNESTO ANTONIO, Ph.D.
Tutor

Firmado electrónicamente por:
ERNESTO ANTONIO
MEDINA DAGGER

Dra. ROJAS CELY CLARA INES , Ph.D.
Miembro No Tutor

CIFUENTES TAFUR, EVELYN CAROLINA
Secretario Ad-hoc

Autoría

Yo, **Anthony Sebastian Ramos Cisneros**, con cédula de identidad 1725075483, declaro que las ideas, juicios, valoraciones, interpretaciones, consultas bibliográficas, definiciones y conceptualizaciones expuestas en el presente trabajo, así como los procedimientos y herramientas utilizadas en la investigación, son de absoluta responsabilidad del autor del trabajo de integración curricular. Así mismo, me acojo a los reglamentos internos de la Universidad de Investigación de Tecnología Experimental Yachay.

Urcuquí, marzo 2020.

Anthony Sebastian Ramos Cisneros
C. I. 1725075483

Autorización de publicación

Yo, **Anthony Sebastian Ramos Cisneros**, con cédula de identidad 1725075483, cedo a la Universidad de Tecnología Experimental Yachay, los derechos de publicación de la presente obra, sin que deba haber un reconocimiento económico por este concepto. Declaro además que el texto del presente trabajo de titulación no podrá ser cedido a ninguna empresa editorial para su publicación u otros fines, sin contar previamente con la autorización escrita de la Universidad.

Asimismo, autorizo a la Universidad para que realice la digitalización y publicación de este trabajo de integración curricular en el repositorio virtual, de conformidad a lo dispuesto en el Art. 144 de la Ley Orgánica de Educación Superior.

Urcuquí, marzo 2020.

Anthony Sebastian Ramos Cisneros

C. I. 1725075483

Acknowledgements

I would like to express my deep gratitude to Ernesto Contreras, for his patient guidance, enthusiastic encouragement and useful critiques of this graduation project. His willingness to give his time so generously has been very much appreciated.

I would also like to extend my thanks to all the professors from the School of Physical Science and Nanotechnology and also to the professors from the School of Mathematical and Computational Sciences for inspiring me by sharing the best of their knowledge and allow me to participate in their research projects. I thank also to all my closest friend for being there in the happy and hard times.

Finally, I wish to thank my parents for their unconditional support and encouragement throughout my studies. I dedicate this first step in my academic career to them.

Resumen

La deformación geométrica mínima (MGD) es un método sistemático y poderoso para extender soluciones isotrópicas bien conocidas a dominios anisotrópicos. Dentro de este marco, el MGD inverso, es decir, el proceso para obtener el sector isotrópico de una solución anisotrópica, se ha estudiado en dimensiones 2 + 1 que revela un tipo de dualidad entre las topologías y / o fuentes de ambos sectores. Para ser más precisos, se ha encontrado que para una solución de agujero negro anisotrópico regular particular que satisface la condición de energía débil, el sector isotrópico obtenido del problema inverso conduce a un agujero negro regular que viola la condición de energía débil, o agujero negro regular que satisface la condición de energía débil. Este proyecto de graduación tiene como objetivo describir la dualidad observada en la aplicación de la MGD inversa en una fuente esférica simétrica dimensional (2+1). Con una solución inicial simétrica esférica anisotrópica general, analizamos el comportamiento de la densidad y la regularidad de la nueva solución obtenida por MGD inversa. Obtuvimos un conjunto de restricciones para satisfacer la positividad de la densidad y un conjunto de restricciones débiles para garantizar la regularidad de las soluciones. Además, se descubrió que la solución de agujero negro BTZ actúa como un límite superior para las restricciones de energía. Después de examinar un caso específico de un comportamiento de dualidad en (2 + 1) dimensiones, presentado en la literatura, mostramos que nuestras limitaciones explican por qué aparece tal dualidad. Finalmente, motivamos un estudio más profundo de la dualidad al estudiar la relación de las condiciones de energía débil y los núcleos de las soluciones, como lo conjetura Dymnikova.

Palabras clave: Relatividad General, MGD, Dualidad, Agujeros Negros.

Abstract

Minimal Geometric Deformation(MGD) is a systematic and powerful method to extend well known isotropic solutions to anisotropic domains. Within this framework, the inverse MGD, namely the process to obtain the isotropic sector of an anisotropic solution, has been studied in 2+1 dimensions revealing a kind of duality between the topologies and/or sources from both sectors. To be more precise, it has been found that for a particular regular anisotropic black hole solution satisfying the weak energy condition, the isotropic sector obtained from the inverse problem leads to either a regular black hole that violates the weak energy condition, or a non-regular black hole that satisfies the weak energy condition. This graduation project aims to describe the duality observed on the application of the inverse MGD in a (2+1) dimensional spherically symmetric source. With a general anisotropic spherical symmetric initial solution, we analyze the behavior of the density and the regularity of the new solution obtained by inverse MGD. We obtained a set of constraints to satisfy the positivity of the density and a set of weak constraints to ensure the regularity of the solutions. Moreover, it was found that the BTZ black hole solution act as an upper bound for the energy constraints. After examining a specific case of a duality behavior in (2+1) dimensions, presented in the literature, we show that our constraints explain why such a duality appears. Finally, we motivate a more deep study of the duality by studying the relation of the weak energy conditions and the cores of the solutions, as it is conjectured by Dymnikova.

Keywords: General Relativity, MGD, Duality, Black Holes.

Contents

List of Figures

List of Tables

Chapter 1

Introduction

General Relativity is one of the main topics in modern physics nowadays and sprang from the idea of Einstein to generalize special relativity. Rather than interpreting space and time as fixed entities as Newton did, he interpreted it as a dynamic space-time that undergoes deformations by the influence of objects with mass/energy. This line of thinking ends in a geometrical interpretation of gravity. Einstein associated the effects of gravity to the curvature of the space-time, instead of to a force. In this sense, he formulated the famous field equations[1],

$$G_{\mu\nu} = \kappa^2 T_{\mu\nu}.$$

These equations, in tensorial notation, explain how the curvature of the space-time changes depending on some matter content. The equations have allowed us to describe several physical phenomena like the perihelion advance of Mercury[2], that was a problem for years; deflexion of light and gravitational lensing[3,4]; gravitational redshift and time delay[5]; and the prediction of black holes and gravitational waves, that were detected recently[6,7]. However, there still exist some fundamental questions that General Relativity cannot answer satisfactorily. For example, the theory cannot give a concise explanation of the existence of dark matter without proposing some unknown matter-energy to reconcile observations with the theory. In the same way, the theory has not been able to explain the observed acceleration of the universe, which is associated with dark energy. Moreover, there is not a convincing quantum formulation of general relativity. These problems have motivated new proposals beyond General Relativity, like $f(R)$ theories, higher curvature theories, Galileon theories, scalar tensors theories, massive gravity, Chern Simons theories, higher spin gravity theories, Horava-Lifshitz gravity, Horndeski's theory, among others.

On the other hand, obtaining new analytical solutions to the Einstein's field equations have been a difficult task, even in (2+1)-dimension. As an example, the coupling of a perfect fluid in a spherically symmetric space-time, with some complex matter-energy to deal with more realistic solutions, leads to technical difficulties due to the non-linearity of the equations[8–11]. In this sense, the Minimal Geometric Deformation (MGD) approach, originally proposed in the context of Randall-Sundrum brane-world[12,13], has been used to study new black hole solutions. MGD has shown to be successfully used to generate brane-world configurations from general relativistic perfect fluid solutions coupling with some other matter content. Even exact and physically acceptable interior solutions had been

found for nonlinear terms following this methodology [14,15].

In addition, MGD has been also used in the inverse context, namely the process of obtaining the isotropic sector of an anisotropic solution. This is the so-called inverse MGD and it was used for the first time to explain the mechanism of formation of exotic matter for wormholes solutions [16]. However, in a specific case of a (2+1) dimensional regular black hole [17] it was found a 'duality' behaviour between the regularity of the topologies and the energy conditions of the sources involved. To be more precise, it has been found that for a particular regular anisotropic black hole solution satisfying the null energy condition, the isotropic sector obtained from the inverse problem leads to either a regular black hole that violates the null energy condition, or a non-regular black hole that satisfies the null energy condition. In this sense, it is conjectured that one of the conditions of the anisotropic solution, i.e. regularity or null energy, is unavoidably violated in the isotropic sector.

1.1 Problem Statement

The lack of understanding of the mechanism by which the duality arises is the problem we aim to tackle in this thesis. We will provide a deep study of the duality between the regularity and the energy conditions for a general (2+1)-dimensional spherically symmetric space-time under gravitational decoupling.

1.2 General and Specific Objectives

The main objective of this graduation project is to explain the duality found in the paper mentioned before [17], and provide general constraints to avoid such a duality.

- In chapter 2, a brief introduction to General Relativity will be presented. Moreover, we will introduce to the general framework of Minimal Geometric Deformation as a tool to find new analytical solutions in general relativity. Finally, the inverse MGD will be explained and an example will be shown.

- In chapter 3, we will provide a general study of the duality, and a set of constraints to satisfy the non-negativity of the density will be proposed as well as the regularity of the solutions.

- In chapter 4, we will presente the conclusions of this graduation project as well as some perspectives for future work.

Chapter 2

Methodology

In this chapter, we summarized all the theoretical background that was used for this graduation project. First, we will start with a brief introduction to General Relativity (GR). The Einstein's field equations (EFE) and solutions in (3+1) and (2+1) gravitational models will be discussed. Later, we will introduce a method to extend solutions in GR using the minimal geometric deformation (MGD) in (3+1) and (2+1). Next, the inverse minimal geometric deformation will be used in a (2+1) dimensional gravity model. Finally, the duality behaviour that has been found in some (3+1) and (2+1) dimensional models [17][16][18] will be summarized.

2.1 General Relativity

In this section, we will give a brief review of the main concepts in GR. We will introduce EFE with their corresponding geometrical and physical interpretation. After that, we will introduce the concept of the energy-momentum tensor and the energy conditions for the solutions of the EFE. Finally, we will presente two of the most relevant solutions for EFE in (3+1) and (2+1) dimensions.

2.1.1 Einstein Field Equations

Albert Einstein proposed his general theory of relativity in 1915[1], as a geometrical model for gravity. He assumed that space-time undergoes deformation in the presence of some matter-energy content, giving rise to gravitational effects. To provide a mathematical interpretation of Einstein's idea, we need to introduce the concept of manifold. A manifold can be thought as a a generalization of what we know as curves or surfaces but in higher dimensions. In particular, in GR, we deal with a four-dimensional manifold *, which corresponds to the space-time, three spatial dimensions plus a temporal dimension. In this sense, it is necessary to equip this manifold with a metric (usually denoted with the letter g), which has the information of the geometric structure of the manifold (Figure. 2.1).

---

*Formally, in general relativity is consider a pseudo-Riemannian manifold, which corresponds to a generalization of a Riemannian manifold because it considers positive, negative and zero-valued metrics [19].
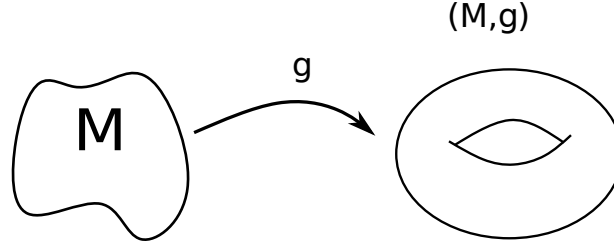
Figure 2.1: Representation of a Manifold *M* with a metric *g*.

Now, we need to tell how this manifold (space-time) will be deformed in the presence of some source of matter-energy. This idea is encoded in the EFE with cosmological constant, written in tensorial notation as

$$G_{\mu\nu} + \Lambda g_{\mu\nu} = \kappa^2 T_{\mu\nu}. \qquad \mu, \nu = 1, 2, 3, 4. \tag{2.1}$$

In these equations: $G_{\mu\nu}$ correspond to the Einstein tensor, which encodes all the information related to the curvature of the given space-time; $T_{\mu\nu}$ is the energy-momentum tensor of a suitable matter model which acts as a source of the gravitational field; Λ is the constant; κ is a proportionality constant that is equal to $\frac{8\pi G}{c}$, where c is the speed of light and G is the gravitational constant. In general, our task is to find the geometry of the manifold (space-time) associated to some matter content. Therefore, we need to solve these equations for the metric tensor $g_{\mu\nu}$.

In these equations, the Einstein tensor is given by

$$G_{\mu\nu} = R_{\mu\nu} + \frac{g_{\mu\nu}}{2} R, \tag{2.2}$$

where *R* corresponds to the Ricci scalar, which is a contraction of the Ricci tensor with the metric,

$$R = g^{\mu\nu} R_{\mu\nu}, \tag{2.3}$$

$R_{\mu\nu}$ corresponds to the Ricci tensor, which is a symmetric tensor given by contraction of the Riemann tensor,

$$R_{\mu\nu} = R^{\alpha}_{\mu\alpha\nu}. \tag{2.4}$$

The Riemann tensor encodes the curvature information of the manifold (space-time) and is given by

$$R^{\rho}_{\sigma\mu\nu} = \partial_\mu \Gamma^{\rho}_{\nu\sigma} - \partial_\nu \Gamma^{\rho}_{\mu\sigma} + \Gamma^{\rho}_{\mu\lambda} \Gamma^{\lambda}_{\nu\sigma} - \Gamma^{\rho}_{\nu\lambda} \Gamma^{\lambda}_{\mu\sigma}, \tag{2.5}$$

where $\Gamma^{\alpha}_{\beta\gamma}$ corresponds to the Christoffel symbols, which are the metric connections. It is important to remark that GR is a torsion-free theory[20] and therefore Christoffel symbols can be written in terms of the metric tensor $g_{\mu\nu}$,

$$\Gamma^{\alpha}_{\mu\nu} = \frac{1}{2} g^{\alpha\theta} (\partial_\mu g_{\theta\nu} + \partial_\nu g_{\theta\mu} - \partial_\theta g_{\mu\nu}). \tag{2.6}$$

Therefore, the left-hand side of the Eq. (2.1) corresponds to a symmetric tensor constructed from derivatives of the metric tensor, while the right-hand side corresponds to a symmetric tensor sourced by certain matter content.
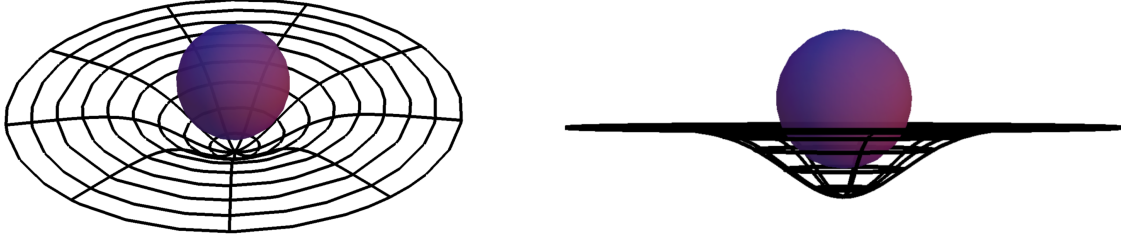
Figure 2.2: Projection of the four dimensional space-time. The black surface correspond to a spherically symmetric representation of space-time and the purple ball represents the matter content that deform such a space-time.

Moreover, due to the symmetries of the tensors, we obtain a set of ten second-order partial differential equations in terms of the metric. The solution to the Eq. (2.1) will provide us the information of the deformation of the space-time given by the matter-energy source as illustrated in Figure. 2.2.

2.1.2   Energy-Momentum Tensor

As we stated before, the energy-momentum tensor encodes the information of the gravitational source. One of the most simple matter model corresponds to the Cauchy Stress Tensor[21] extended to curved four-dimensional space-time. In particular, for a perfect fluid, it is given by

$$\left[T^{\mu}_{\nu}\right] = \begin{pmatrix} -\rho & 0 & 0 & 0 \\ 0 & P & 0 & 0 \\ 0 & 0 & P & 0 \\ 0 & 0 & 0 & P \end{pmatrix}, \tag{2.7}$$

which in tensorial notation, it read as

$$T_{\mu\nu} = \left(\rho + \frac{P}{c^2}\right)U_\mu U_\nu + P g_{\mu\nu}, \tag{2.8}$$

where ρ corresponds to the density, P corresponds to the pressure and U_μ corresponds to the four-velocity in co-moving coordinates[22]. An important aspect of the four-dimensional energy-momentum tensor is that it has to satisfy the conservation law in curved space-time defined as

$$\nabla_\mu T^{\mu\nu} = 0, \tag{2.9}$$

where ∇_μ corresponds to the covariant derivative defined as

$$\nabla_\sigma T^{\nu_1\mu_2\cdots\mu_k}_{\nu_1\nu_2\cdots\nu_j} = \partial_\sigma T^{\nu_1\mu_2\cdots\mu_k}_{\nu_1\nu_2\cdots\nu_j} + \Gamma^{\nu_1}_{\sigma\lambda}T^{\lambda\mu_2\cdots\mu_k}_{\nu_1\nu_2\cdots\nu_j} + \Gamma^{\nu_2}_{\sigma\lambda}T^{\mu_1\lambda\cdots\mu_k}_{\nu_1\nu_2\cdots\nu_j} + \cdots - \Gamma^{\lambda}_{\sigma\nu_1}T^{\mu_1\mu_2\cdots\mu_k}_{\lambda\nu_2\cdots\nu_j} - \Gamma^{\lambda}_{\sigma\nu_2}T^{\mu_1\mu_2\cdots\mu_k}_{\nu_2\lambda\cdots\nu_j} - \cdots . \tag{2.10}$$

An example of covariant derivative, for a (1,1) rank tensor [†]

$$\nabla_\alpha V^\alpha_\beta = \partial_\alpha V^\alpha_\beta + \Gamma^\beta_{\alpha\lambda} V^\lambda_\beta - \Gamma^\lambda_{\alpha\beta} V^\alpha_\lambda, \tag{2.11}$$

The conservation law means that for the $\nu = 0$ component, the energy is conserved and for $\nabla_k T^{\mu k}$, $k = 1, 2, 3$ the *kth* components of the momentum are conserved, and it corresponds to a fundamental physical law that we should satisfy to ensure that we are dealing with a physical relevant solution. Finally, it is worth mentioning that there is a more general way to build an energy-momentum tensor based on the Lagrangian formulation (see Appendix A for more details).

2.1.3   Energy Conditions

Until now we know that EFE provides us with information about the space-time that is deformed by some matter content, which corresponds to the energy-momentum tensor. Moreover, we know that the energy-momentum tensor satisfies the conservation laws. However, we should impose some extra constraints on the energy-momentum tensor in order to know if a solution is or not physically relevant. In this sense, given an energy-momentum tensor $T_{\mu\nu}$, we classified the energy conditions as follows:

- **Null Energy Condition** (NEC), this energy condition is given by

$$T_{\mu\nu} V^\mu V^\nu \geq 0, \tag{2.12}$$

  where V^μ are null vectors. It means that the matter-energy density observed by a null observer is always positive.

- **Weak Energy Condition** (WEC), which is given by

$$T_{\mu\nu} U^\mu U^\nu \geq 0, \tag{2.13}$$

  where U^μ are time-like vector. This means that the matter-energy density observed by the corresponding observers is always non-negative. Notice that due to null vectors are limits of the time-like vectors, the WEC implies the NEC [22].

- **Strong Energy Condition** (SEC) is given by

$$T_{\mu\nu} U^\mu U^\nu \geq \frac{1}{2} T^\lambda_\lambda U^\sigma U_\sigma \tag{2.14}$$

  for all time-like vectors U^μ [23].

[†]The rank (k, l) refer to the total number of contravariant and covariant indices of the tensor, respectively.

If we consider a perfect fluid, then the expression (2.13) for the WEC reduces to

$$\rho \geq 0 \qquad \rho + p \geq 0 \text{ (NEC)}, \tag{2.15}$$

which are simply the reasonable requirements for the energy density to be non-negative, to avoid exotic matter, and for the pressure to be not too large compared to the energy density.

Moreover, the SEC (2.14) for a perfect fluid becomes

$$\rho + p \geq 0 \quad \text{and} \quad \rho + 3p \geq 0 \tag{2.16}$$

2.1.4 Schwarzschild Exterior Solution

The first exact solution to the EFE was found by Karl Schwarzschild in 1916[24]. Schwarzschild solved EFE (2.1) for a spherically symmetric, vacuum, asymptotically flat space-time. Mathematically these assumptions become

$$T^{\mu\nu} = 0, \qquad\qquad\qquad\qquad \text{Vacuum} \tag{2.17}$$

$$\partial_t g_{\mu\nu} = 0, \qquad\qquad\qquad\qquad \text{Stationary} \tag{2.18}$$

$$ds^2 = -A(r)dt^2 + B(r)dr^2 + r^2 \left[d\theta^2 + \sin(\theta)^2 d\phi^2 \right], \qquad \text{Spherically Symmetric} \tag{2.19}$$

where the last equation corresponds to the line element, which encodes the information of the metric tensor in the following form

$$ds^2 = g_{ij}dx^i dx^j, \tag{2.20}$$

and signature $(-, +, +, +)$. Therefore the expression for the metric tensor for our case becomes

$$\left[g_{\mu\nu} \right] = \begin{bmatrix} -A(r) & 0 & 0 & 0 \\ 0 & B(r) & 0 & 0 \\ 0 & 0 & r^2 & 0 \\ 0 & 0 & 0 & r^2 \sin(\theta)^2 \end{bmatrix}. \tag{2.21}$$

It is important to remark that A and B do not depend on θ and ϕ because it would break the spherical symmetry of the solutions. Also, they do not depend on time because we are considering stationary solutions. Another important feature is that we are considering asymptotically flat solutions, it means that for $r \to \infty$ our curved metric becomes the metric of the Minkowski space

$$ds^2_{Minkowski} = -c^2 dt^2 + dr^2 + r^2 \left[d\theta^2 + \sin(\theta)^2 d\phi^2 \right], \tag{2.22}$$

this implies that

$$\lim_{r \to \infty} A(r) = c^2, \tag{2.23}$$

$$\lim_{r \to \infty} B(r) = 1. \tag{2.24}$$

Now, if we consider Eq. (2.1) with the assumptions (2.17), the EFE read

$$G_{\mu\nu} = 0. \tag{2.25}$$

Now, if we contract the equation with the metric tensor $g^{\mu\nu}$ we obtain

$$g^{\mu\nu}R_{\mu\nu} - \frac{1}{2}g^{\mu\nu}g_{\mu\nu}R = 0, \tag{2.26}$$

which reduces to

$$R = 0. \tag{2.27}$$

Finally, Eq. (2.25) reduce to solve

$$R_{\mu\nu} = 0. \tag{2.28}$$

Now, let us compute the non vanishing components of the Christoffel symbols

$$\Gamma^1{}_{12} = \frac{\nu'(r)}{2}, \qquad\qquad\qquad \Gamma^1{}_{21} = \frac{\nu'(r)}{2}, \tag{2.29}$$

$$\Gamma^2{}_{11} = \frac{1}{2}e^{\nu(r)-\lambda(r)}\nu'(r), \qquad\qquad \Gamma^2{}_{22} = \frac{\lambda'(r)}{2}, \tag{2.30}$$

$$\Gamma^2{}_{33} = r\left(-e^{-\lambda(r)}\right), \qquad\qquad \Gamma^3{}_{23} = \frac{1}{r}, \tag{2.31}$$

$$\Gamma^3{}_{32} = \frac{1}{r}, \tag{2.32}$$

from which the Ricci tensor components read as

$$R_{11} = \frac{A''(r)}{2B(r)} - \frac{A'(r)B'(r)}{4B(r)^2} - \frac{A'(r)^2}{4A(r)B(r)} + \frac{A'(r)}{rB(r)}, \tag{2.33}$$

$$R_{22} = -\frac{A''(r)}{2A(r)} + \frac{A'(r)B'(r)}{4A(r)B(r)} + \frac{A'(r)^2}{4A(r)^2} + \frac{B'(r)}{rB(r)}, \tag{2.34}$$

$$R_{33} = -\frac{rA'(r)}{2A(r)B(r)} + \frac{rB'(r)}{2B(r)^2} - \frac{1}{B(r)} - \cot^2(\theta) + \csc^2(\theta), \tag{2.35}$$

$$R_{44} = -\frac{r\sin^2(\theta)A'(r)}{2A(r)B(r)} + \frac{r\sin^2(\theta)B'(r)}{2B(r)^2} - \frac{\sin^2(\theta)}{B(r)} + \sin^2(\theta). \tag{2.36}$$

Notice that $R_{44} = \sin(\theta)^2 R_{33}$. Then, wen can only consider (2.33), (2.34) and (2.35) as independent equations. However, we have three equations and two unknowns. Thus, let us multiply $\frac{B(r)}{A(r)}$ to (2.33) and sum (2.34)

$$\frac{1}{r}\left[\frac{A'(r)}{A(r)} + \frac{B'(r)}{B(r)}\right] = 0, \tag{2.37}$$

solving the ODE (2.37), we obtain

$$B(r) = \frac{c_1}{A(r)}, \tag{2.38}$$

replacing (2.38) into (2.35), we obtain

$$-\frac{rA'(r) + A(r) - c_1}{c_1} = 0, \tag{2.39}$$

solving the ODE we get,

$$A(r) = c_1 + \frac{c_2}{r}. \tag{2.40}$$

Now, we have two constants c_1 and c_2 that need to be adjusted with the extra conditions for our solutions. First, let consider the asymptotically flat condition (2.23) for $A(r)$

$$\lim_{r \to \infty} A(r) = c_1 \tag{2.41}$$

therefore $c_1 = c^2$, where c^2 is the squared speed of light. We can rewrite $A(r)$ as

$$A(r) = c^2 \left(1 + \frac{c_3}{r} \right), \tag{2.42}$$

where $c_3 = \frac{c_2}{c^2}$. Then, it is clear that the condition (2.24) for $B(r)$ is satisfied

$$\lim_{r \to \infty} B(r) = \frac{c^2}{c^2} = 1. \tag{2.43}$$

For c_3, we need to consider the weak field limit in which the EFE equations reduces to the Newtonian limit, namely

$$g_{00} = \eta_{00} + h_{00}, \tag{2.44}$$

where $\eta_{00} = -c^2$ and correspond to the Minkowskian metric $\eta_{\mu\nu}$ and $h_{00} = \frac{2\Phi}{c^2}$, with $\Phi = \frac{GM}{r}$ that corresponds to the gravitational field potential[23]. Then, our equation for $A(r)$ becomes

$$g_{00} = -A(r) = -c^2 \left(1 + \frac{c_3}{r} \right) = -c^2 + \frac{2GM}{r}, \tag{2.45}$$

from where we identify $c_3 = -\frac{2GM}{c^2}$. Thus, we obtain that

$$A(r) = c^2 \left(1 - \frac{2GM}{c^2 r} \right) \quad \text{and} \quad B(r) = \frac{1}{\left(1 - \frac{2GM}{c^2 r} \right)}. \tag{2.46}$$

Finally, Schwarzschild solution reads

$$ds^2 = -c^2 \left(1 - \frac{2GM}{c^2 r} \right) dt^2 + \frac{1}{\left(1 - \frac{2GM}{c^2 r} \right)} dr^2 + r^2 (d\theta^2 + \sin(\theta)^2 d\phi^2). \tag{2.47}$$

This solution allows to describe exterior solutions and the trajectory followed by particles like the perihelion advance of Mercury[2] and the deflexion of light and gravitational lensing[3,4].

Event Horizon and Singularities.

Now, let us study some of the physical implications of the Schwarzschild solution. First, it is worth noticing that this solution has two critical values r_s and r_h for which our solution has a divergent behaviour. For $r_s = 0$, the time component of the metric reads

$$-c^2 \left(1 - \frac{2GM}{c^2 r}\right) \to \infty,$$

and for $r_h = \frac{2GM}{c^2}$, the radial part reads

$$\frac{1}{\left(1 - \frac{2GM}{c^2 r}\right)} \to \infty.$$

In order to study this divergent behaviour of the solutions, we need to define regularity. In this work, regularity refers to non-divergent curvature scalar[23]. We can consider curvature scalars like Ricci scalar, Ricci squared saclar, Kretschmann scalar, among others. In particular, it is well known that for the Schwarzschild solution the Ricci curvature scalar vanishes because of (2.26), and the only non-vanishing scalar is the Kretschmann scalar given by

$$\mathcal{K} = R_{abcd} R^{abcd} = \frac{48 G^2 m^2}{c^4 r^6}, \tag{2.48}$$

from where is clear that at $r_h = \frac{2GM}{c2}$, $\mathcal{K}$ is just a constant and does not diverge. In this context, this critical value corresponds to the so called *Event Horizon*. In order to understand the behaviour at the event horizon, we are going to consider null geodesics for fixed θ and ϕ, in our solution,

$$ds^2 = 0 \quad \Leftrightarrow \quad \left(1 - \frac{2MG}{c^2 r}\right) dt^2 - \left(\frac{1}{1 - \frac{2MG}{c^2 r}}\right) dr^2 = 0, \tag{2.49}$$

solving this differential equation, we obtain

$$t_{\pm} = \pm \left(r + 2MG \ln |r - 2MG|\right). \tag{2.50}$$

In this case, t_+ corresponds to outgoing lines (Red), and the t_- corresponds to the ingoing lines (Blue) as it is shown in Figure. 2.3. Given that our pseudo Riemannian manifold must coincides with the Minkowskian spacetime in a small neighborhood, we define that the intersection of the ingoing and outgoing lines defines a null cone in a small region (green cone) that will define the causal future and the causal past of the event located at the intersection, as it is observed in the Figure. 2.3. Besides, for $r < r_h$ the causal future of the null cone point directly to r_s, which means that a particle will unavoidably go to r_s. On the other hand for $r > r_h$ the causal future of our null cone tell us that we can avoid going to the point r_h, and consequently to r_s. It is worth mentioning that the point $r = r_s = 0$ is not defined for these null geodesics, which means that the geometry at this point is "broken" and classically the behaviour is unknown at this point. Notice that in this coordinate system the null geodesics asymptotically approach to the event horizon r_h but it never reach the point. However, this is just a misinterpretation of coordinates and it can be demonstrated that a test particle not only reach the event horizon but traverses it. Indeed, if we perform a change of coordinate we can study the behaviour of the solution at r_h. For this purpose we are going to consider the
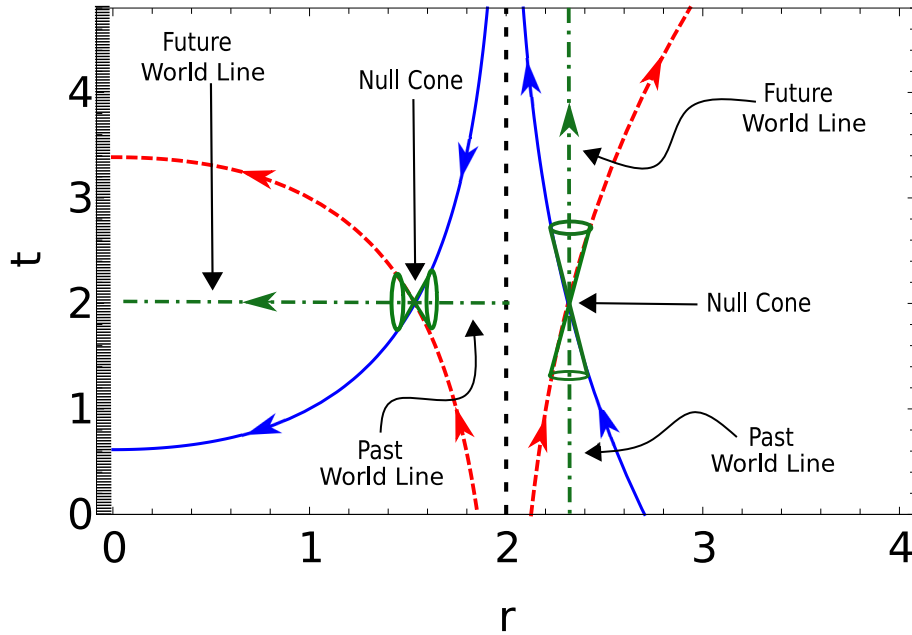
Figure 2.3: Plot of the null geodesics for fixed θ, ϕ and $M = G = c = 1$. (Blue) lines corresponds to the ingoing lines t_-. (Red) lines corresponds to the outgoing lines t_+. The event horizon in this case is located at $r_h = 2$

Eddington-Finkelstein[25,26] change of coordinates, obtaining

$$\tilde{t}_- = -r + C_1, \qquad \text{(Ingoing)} \qquad (2.51)$$

$$\tilde{t}_+ = r + 4MG \ln |r - 2MG|. \qquad \text{(Outgoing)} \qquad (2.52)$$

In this new coordinate system, it is observed that r_h corresponds to a null surface (Figure. 2.4). If we study the behaviour of the causal future of the null cone for $r < r_h$, again, we observe that unavoidably a test particle will go directly to the $r_s = 0$ as it is observed in Figure. 2.4, in contrast to $r > r_h$, where a test particle could "escape" and avoid the undefined point r_s. The behaviour of this null surface located at $r = r_h$ is like an unidirectional membrane, where if a test particle goes through it, it will never go out.
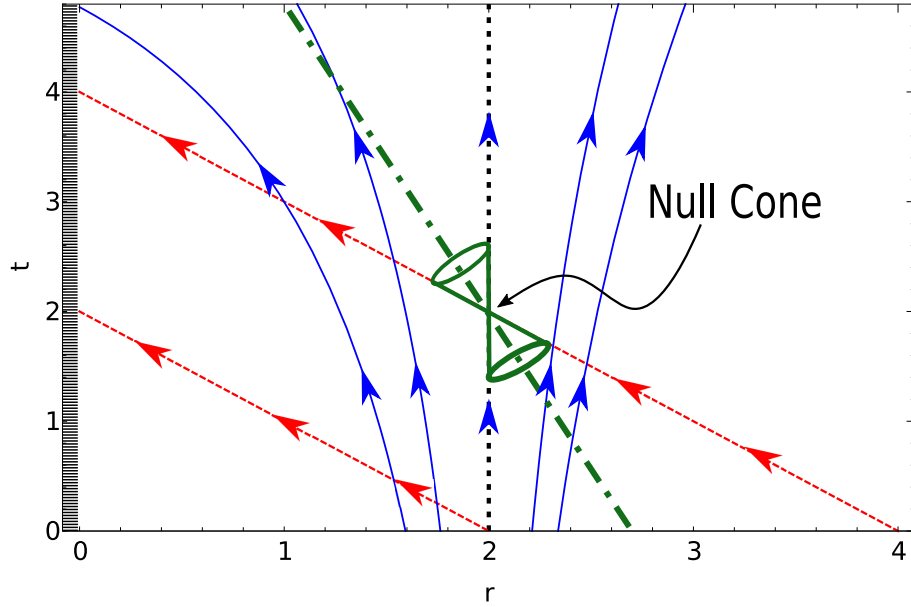
Figure 2.4: Plot of the null geodesics for fixed θ, ϕ and $M = G = c = 1$ for Eddington-Frinklestein coordinate system. (Blue) lines corresponds to the ingoing lines $\tilde{t}_-$. (Red) lines corresponds to the outgoing lines $\tilde{t}_+$. The event horizon in this case is located at $r_h = 2$

Now, let us consider the behaviour near the point $r_s = 0$, which is located inside this uni-dimensional membrane at r_h. After evaluating the Kretschmann scalar (2.48) at the limit of $r \rightarrow r_s$, we obtain

$$\lim_{r \rightarrow r_s} \mathcal{K} = \infty,$$

showing a divergent behaviour of the scalar at r_s and, therefore, the solution is irregular. We call this point *singularity* (Figure. 2.5). Solutions that have a null surface enclosing a singularity are called *Black Hole* solutions. It is worth mentioning that in the case that the solution have at least one null surface with no singularity inside the membrane is called *Regular Black Hole* solution. Otherwise, in the case that there is a singularity outside the null surface or without a null surface, it is called *Naked Singularity* and it is a non-physical solution[27].
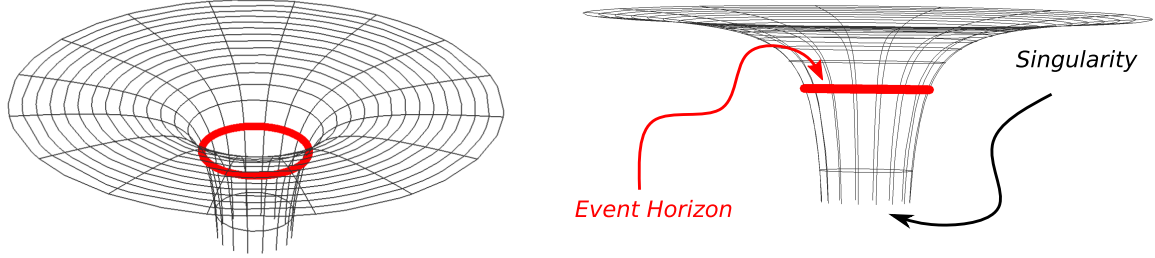
Figure 2.5: Schwarzschild black hole solution representation of the radial and temporal part. Black lines corresponds to the representation of the solution for a spherically symmetric space-time. Red line correspond to the representation of the null surface located at r_h or the *event horizon*. The undefined region at the center of the surface corresponds to the *singularity* r_s that is never reached.

2.1.5 BTZ Solution

Low dimensional gravity, and in particular (2+1) dimensional models has been used to study toy models that give some insight for problems of its (3+1) dimensional counterpart. One of its solutions is the so called BTZ black hole solution [28]. The acronym BTZ comes from the authors of the paper Máximo Bañados, Claudio Teitelboim and Jorge Zanelli. The solution to Eq. (2.1) in (2+1) dimensions with a negative cosmological constant and assuming circularly symmetric spacetimes corresponds to

$$ds^2 = -N^2(r)dt^2 + \frac{1}{N^2(r)}dr^2 + r^2(N^\phi dt + d\phi)^2, \tag{2.53}$$

where $N(r)^2$ stands for the squared lapse and $N^\phi(r)$ to the angular shift, and are given by

$$N^2(r) = -M + \frac{r^2}{\ell^2} + \frac{J^2}{4r^2}, \qquad N^\phi(r) = -\frac{J}{2t^2}. \tag{2.54}$$

The integration constants M and J correspond to the mass and angular momentum, respectively. Now, let us focus on the physical meaning of this solution. First, notice that the function $N(r)$ has two roots for r given by

$$r_\pm = \ell \left\{ \frac{M}{2} \left[1 \pm \left(1 - \left(\frac{J}{M\ell} \right)^2 \right)^{\frac{1}{2}} \right] \right\}^{\frac{1}{2}}, \tag{2.55}$$

r_+ corresponds to the black hole horizon. This suggests that we must have

$$M > 0, \qquad |J| \le M\ell,$$

to ensure the existence of the horizon. Here ℓ provides a length scale necessary to have a horizon in a theory in which the mass is dimensionless [28]. Moreover, for $\ell >> 1$ the black hole exterior is pushed to infinity. From the expression

of $N^2(r)$ in (2.54), for $M \to 0$ and $J \to 0$ the horizon disappear (Figure. 2.6), just as the curvature singularity of a negative mass black hole in 3+1 dimensions [28]. On the other hand, for $M = -1$ and $J = 0$ no real roots appear for $N^2(r)$ (Figure. 2.6).

Figure 2.6: Squared lapse versus r, with $J = 0$ and $\ell = 3$. (Blue) correspond to $M = 0$ naked singularity at $r_+ = 0$. (Red) correspond to $M = 1$ horizon at $r_+ = 3$. (Green) correspond to $M - 1$ no singularity neither horizon.

In addition, we can observe that the configuration of the line element for the case of $J = 0$ reads

$$ds^2 = -\left[-M + \left(\frac{r}{\ell}\right)^2\right] dt^2 + \frac{1}{\left[-M + \left(\frac{r}{\ell}\right)^2\right]} dr^2 + r^2 d\phi^2, \tag{2.56}$$
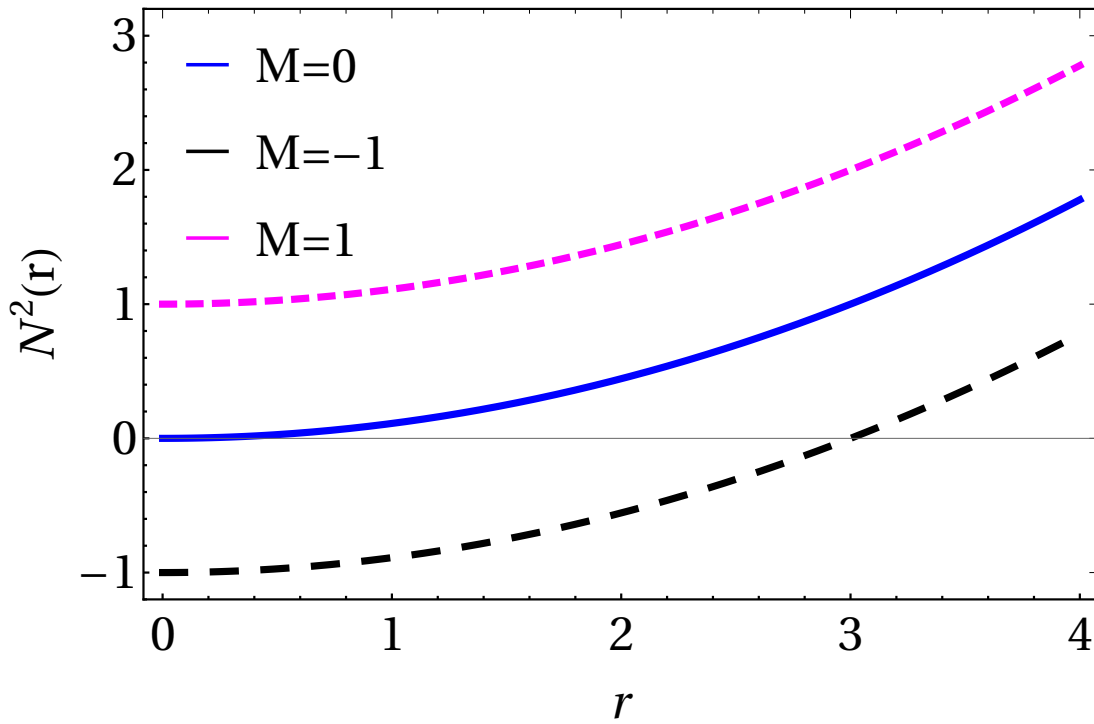
computing the curvature scalars for the case of $J = 0$ near the roots of $N^2(r)$, we obtain

$$R = -\frac{6}{\ell^2}, \tag{2.57}$$

$$\mathcal{K} = \frac{12}{\ell^4}. \tag{2.58}$$

For both cases the curvature scalars are constant, even for $r = 0$. This could suggest that our solution corresponds to a regular solution. However, in the origin the solution is not well behaved in the sense that it is geodesically incomplete and require a deeper study [28] which is out of the scope of this work.

2.2 Minimal Geometric Deformation

In this section, we will give an introduction to Minimal Geometric Deformation (MGD) method, for (3+1) and (2+1) dimension, as a tool to extend isotropic solutions coupled to some extra source to anisotropic domains. After that, the inverse method will be introduced in the context of (2+1) dimensional gravity.

2.2.1 Deformation in (3+1) dimensional Gravity

The task of solving the EFE analytically has become in one of the main problems in General Relativity due to the non-linearity of the differential equations, even in (2+1) dimensions. As we stated before, when we consider a spherically symmetric space-time with a perfect fluid source [8][9][10], which is coupled with some complex matter-energy to describe more realistic scenarios, the system becomes almost impossible to solve analytically [29][11]. Consequently, MGD, which was originally proposed in the context of Randall-Sundrum brane-world [12][13], was extended to investigate new black hole solutions [30][31]. MGD has been successfully used to obtain exact and physically acceptable solutions for spherically symmetric interior stellar distributions [32][33]; to prove the consistency of a Schwarzschild exterior [34]; to derive bounds on extra-dimensional parameters [35]; to investigate the gravitational lensing phenomena beyond GR [36]; among others.

Einstein's Field Equations for Multiple Sources

Here we will provide a description of the method. For simplicity, we are going to consider that $G = c = 1$. First, let us consider EFE for spherical symmetry space-time and a general source $T_{\mu\nu}^{(tot)}$ given by

$$T_{\mu\nu}^{(tot)} = T_{\mu\nu}^{(m)} + \alpha \theta_{\mu\nu}, \tag{2.59}$$

then our EFE with cosmological constant Λ (2.1) become

$$G_{\mu\nu} + \Lambda g_{\mu\nu} = -\kappa^2 T_{\mu\nu}^{(tot)}, \tag{2.60}$$

where $T_{\mu\nu}^{(m)}$ corresponds to the energy-momentum tensor for a perfect fluid (2.8) given by

$$T_{\mu\nu}^{(m)} = (\rho + p)\, U_\mu U_\nu - p g_{\mu\nu}. \tag{2.61}$$

Here $\theta_{\mu\nu}$ in (2.59) corresponds to any additional source of gravity which is coupled with $T_{\mu\nu}^{(m)}$ and α is a constant relating the strength of the coupling. This extra source is the one that will generate anisotropies in our initial self-gravitating system. Further, it is important to remark that our $T_{\mu\nu}^{(tot)}$ should satisfy the conservation equation given that our EFE are divergence-free, then

$$\nabla_\nu T_\mu^{(tot)\nu} = 0, \tag{2.62}$$

which reads as

$$\nabla_\nu T_1^{(tot)\nu} = \left[p' + \frac{\nu'}{2}(p + \rho) \right] + \alpha \left[\left(\theta_1^1\right)' - \frac{\nu'}{2}\left(\theta_0^0 - \theta_1^1\right) - \frac{2}{r}\left(\theta_2^2 - \theta_1^1\right) \right] = 0. \tag{2.63}$$

The first bracket corresponds to $\nabla_\mu T_1^{(m)\mu}$ of the isotropic fluid and the second bracket corresponds to $\nabla_\mu \theta_1^\mu$ of the coupled source. Thus, we can rewrite the conservation law as

$$\nabla_\mu T_\nu^{(tot)\mu} = \nabla_\mu T_\nu^{(m)\mu} + \alpha \nabla_\mu \theta_\nu^\mu = 0, \tag{2.64}$$

Notice that the conservation law is satisfied independently for the sectors, it means that the perfect fluid and the extra source do not exchange their energy-momentum tensor, and they only interact gravitationally.

Now, let us consider the Schwarzschild-like coordinates line elements

$$ds^2 = -e^{\nu(r)} dt^2 + e^{\lambda(r)} dr^2 + r^2 \left[d\theta^2 + \sin(\theta)^2 d\phi^2 \right], \tag{2.65}$$

for $r \in [0, R]$, where R is the radius of the soruce; and the fluid 4-velocity is given by $U^\mu = e^{-\frac{\nu}{2}} \delta_0^\mu$. If we replace the metric (2.65) into the EFE with mixed notation (2.60), we obtain

$$G_\nu^\mu + \Lambda \delta_\nu^\mu = k^2 T_\nu^{(tot)\mu}, \tag{2.66}$$

expanding (2.66), the following system of differential equations is obtained

$$-\kappa^2(\rho + \alpha\theta_0^0) = -\frac{1}{r^2} + \Lambda + e^{-\lambda}\left(\frac{1}{r^2} - \frac{\lambda'}{r}\right), \tag{2.67}$$

$$\kappa^2(p + \alpha\theta_1^1) = -\frac{1}{r^2} + \Lambda + e^{-\lambda}\left(\frac{1}{r^2} + \frac{\nu'}{r}\right), \tag{2.68}$$

$$\kappa^2(p + \alpha\theta_2^2) = \Lambda + \frac{e^{-\lambda}}{4}\left(2\nu'' + \nu'^2 - \lambda'\nu' + 2\frac{\nu' - \lambda'}{r}\right), \tag{2.69}$$

where, $f' = \partial_r f$. Note that perfect fluid is recovered when $\alpha \to 0$.

The system (2.67)-(2.69) have seven unknown functions $\left\{\nu(r), \lambda(r), \rho(r), p(r), \theta_{\mu\nu}\right\}$. Besides, we can rewrite the energy-momentum tensor in terms of effective quantities $T_{\nu}^{(tot)\mu} = diag(-\tilde{\rho}, \tilde{p}_r, \tilde{p}_t, \tilde{p}_t)$, where

$$\tilde{\rho} = \rho + \alpha\theta_0^0; \tag{2.70}$$

$$\tilde{p}_r = p + \alpha\theta_1^1; \tag{2.71}$$

$$\tilde{p}_t = p + \alpha\theta_2^2. \tag{2.72}$$

These new effective expressions show that the source $\theta_{\mu\nu}$ could, in general, induce an anisotropy, which by subtracting (2.71) and (2.72) can be expressed as

$$\Pi \equiv \tilde{p}_t - \tilde{p}_r = \alpha(\theta_1^1 - \theta_2^2). \tag{2.73}$$

Therefore, the system of Eqs (2.67)-(2.69) can be considered as an anisotropic fluid[37].

Gravitational decoupling by MGD

Now, let us implement the MGD in order to solve the system (2.67)-(2.69). First, let us consider the following geometric deformation to the metric (2.65)

$$\nu(r) = \xi(r) + \alpha g(r), \tag{2.74}$$

$$e^{-\lambda(r)} = \mu + \alpha w(r), \tag{2.75}$$

where $g(r)$ and $w(r)$ are the deformations undergone by the time and radial parts of the metric, respectively. In this sense, the minimal geometric deformation correspond to the specific case where $g \to 0$. Thus, we can separate the EFE and identify three sectors.

1. **Isotropic Sector** that corresponds, in this case, to a perfect fluid with $\alpha = 0$ and $\xi(r) = \nu(r)$, whose metric is given by

$$ds^2 = -e^{\nu(r)}dt^2 + \frac{1}{\mu(r)}dr^2 + r^2\left[d\theta^2 + \sin(\theta)^2\right], \tag{2.76}$$

and the EFE read

$$\kappa^2\rho = \frac{1}{r^2} - \Lambda - \frac{\mu}{r^2} - \frac{\mu'}{r}, \tag{2.77}$$

$$\kappa^2 p = -\frac{1}{r^2} + \Lambda + \mu\left(\frac{1}{r^2} + \frac{\nu'}{r}\right), \tag{2.78}$$

$$\kappa^2 p = \Lambda + \frac{1}{4}\mu'\left(\nu' + \frac{2}{r}\right) + \frac{1}{4}\mu\left[2\nu'' + (\nu')^2 + \frac{2\nu'}{r}\right], \tag{2.79}$$

along with the conservation equation $\nabla_\nu T_\mu^{(m)\nu} = 0$, which reduces to

$$p' + \frac{\nu}{2}(\rho + p) = 0. \tag{2.80}$$

2. **Decupler Sector** that corresponds to the system with the source $\theta_{\mu\nu}$,

$$\kappa^2\theta_0^0 = -\frac{w'}{r} - \frac{w}{r^2}, \tag{2.81}$$

$$\kappa^2\theta_1^1 = w\left(\frac{\nu'}{r} + \frac{1}{r^2}\right), \tag{2.82}$$

$$\kappa^2\theta_2^2 = \frac{1}{4}w\left[2\nu'' + (\nu')^2 + \frac{2\nu'}{r}\right] + \frac{1}{4}w'\left(\nu' + \frac{2}{r}\right), \tag{2.83}$$

The equations (2.81)-(2.83) look very similar to the standard spherically symmetric EFE for an anisotropic fluid with energy-momentum tensor $\theta_{\mu\nu}$. However, the right-hand side of (2.81) and (2.82) had a missing term $-\frac{1}{r^2}$. This inconvenient can be solved by considering as a source

$$\kappa^2\Theta_\mu^\nu := \kappa^2\theta_\mu^\nu + \frac{1}{r^2}\left(\delta_\mu^0\delta_0^\nu + \delta_\mu^1\delta_1^\nu\right). \tag{2.84}$$

Therefore, the equations will correspond to the spherically symmetric EFE for a anisotropic fluid, whose metric is given by

$$ds^2 = -e^{\nu(r)}dt^2 + \frac{1}{w(r)}dr^2 + r^2\left[d\theta^2 + \sin(\theta)^2 d\phi^2\right]. \tag{2.85}$$

3. **Total Sector** that corresponds to the sum of both sectors, whose metric is given by

$$ds^2 = -e^{\nu(r)}dt^2 + \frac{1}{\mu + \alpha w(r)}dr^2 + r^2\left[d\theta^2 + \sin(\theta)^2 d\phi^2\right]. \tag{2.86}$$

and the EFE correspond to

$$-\kappa^2(\rho + \alpha\theta_0^0) = \Lambda + \frac{r(\mu' + \alpha w') - 1}{r^2} + \frac{\mu + \alpha w}{r^2}, \tag{2.87}$$

$$\kappa^2(p + \alpha\theta_1^1) = \Lambda + \frac{(r\nu' + 1)(\mu + \alpha w)}{r^2} - \frac{1}{r^2}, \tag{2.88}$$

$$\kappa^2(p + \alpha\theta_2^2) = \Lambda + \frac{(r\nu' + 2)(\mu' + \alpha w')}{4r} + \frac{[2r\nu'' + \nu'(r\nu' + 2)](\mu + \alpha w)}{4r}, \tag{2.89}$$

Consequently, MGD allow us to separate an unknown system (2.67) - (2.69) into a set of equations for a prefect fluid (2.77)-(2.79) $\{\rho, p, \mu, \nu\}$ plus a system with four unknown functions for the decouple sector (2.81) - (2.83) $\{w, \theta_0^0, \theta_1^1, \theta_2^2\}$. In this sense, if we consider a known isotropic solution (i.e, $\{\rho, p, \mu, \nu\}$ are known functions), and an equation of state (2.73), we obtain a system with three unknowns $\{w, \theta_0^0, \theta_1^1\}$ for the decoupler sector (2.81) - (2.83), that could be solved analytically. Finally, we sum both solutions obtaining (2.67) - (2.69), which correspond to the new anisotropic solution.

In this section, we have shown that given a well known perfect fluid solution it can be extended to anisotropic domains by performing a deformation in the radial part of the metric, and adding an extra source, that interacts gravitationally (Figure. 2.7). As a final remark, this method can be extended considering any kind of seed initial solution, even an anisotropic solution.
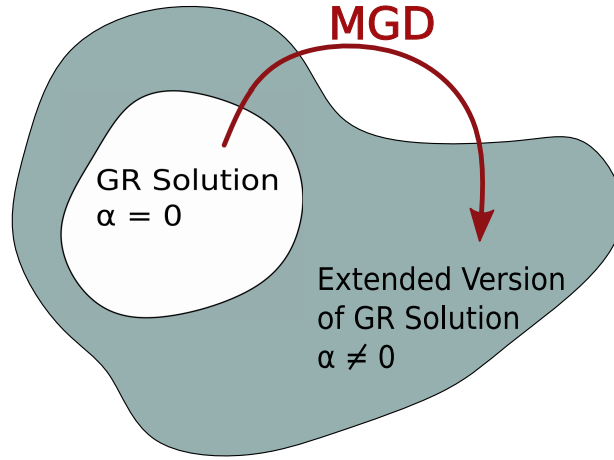
Figure 2.7: Representation of how a GR solution is forced to be a solution in the new gravitational sector by MGD, the α represents the constant that controls the deformation

2.2.2 Minimal Geometric Deformation in (2+1) dimensional Gravity

Three dimensional gravity still represents an important source for theoretical developments like identification of cosmic strings solutions with topological defects in two-dimensional condensed matter systems as graphene layers[38][39]. Furthermore, it has been shown that 2+1 dimensional black holes have the same conceptual foundations as realistic 3+1 dimensional general relativity theories[28]. Even more, one can actually write down viable candidates for a quantum theory with (2+1) dimensional gravitational theories, as an example is the BTZ black hole that has been found to be dual to a Chern Simmons theory SU(2,2)[40][41]. In this sense, (2+1) dimensional gravity has become an active field of research, drawing insight from General Relativity, differential geometry, topology, particle physics and topological field theory[42][43]. Therefore, it is also important to obtain the MGD version for a (2+1) dimensional gravity, which was introduced for the first time in[44].

Obtaining the MGD for a (2+1) dimensional gravity it is almost trivial after the previous derivation in (3+1) dimensional gravity. So, let us consider the EFE with cosmological constant for (2+1) dimension

$$G_\nu^\mu + \Lambda g_\nu^\mu = k^2 T_\nu^{(tot)\mu}, \qquad \mu, \nu = 0, 1, 2, \tag{2.90}$$

where the total energy-momentum tensor as before is given by

$$T_\nu^{(tot)\mu} = T_\nu^{(m)\mu} + \theta_\nu^\mu. \tag{2.91}$$

In this case, $T_\nu^{(m)\mu} = diag(-\rho, p, p)$ stands for the energy-momentum tensor of a perfect fluid and $\theta_\nu^\mu = diag(-\rho^\theta, p_r^\theta, p_\perp^\theta)$ contain the information of the decouple matter. So, let us consider the spherically symmetric space-time with the following line element

$$ds^2 = -e^{\nu(r)}dt^2 + e^{\lambda(r)}dr^2 + r^2 d\phi^2 \tag{2.92}$$

Then, replacing (2.92) in (2.91), we obtain

$$\kappa^2 \tilde{\rho} = -\Lambda + \frac{e^{-\lambda}\lambda'}{2r}, \tag{2.93}$$

$$\kappa^2 \tilde{p}_r = \Lambda + \frac{e^{-\lambda}\nu'}{2r}, \tag{2.94}$$

$$\kappa^2 \tilde{p}_\perp = \Lambda + \frac{1}{4}e^{-\lambda}\left(-\lambda'\nu' + 2\nu'' + \nu'^2\right), \tag{2.95}$$

where the effective density and pressures are given by

$$\tilde{\rho} = \rho + \alpha\rho^\theta, \tag{2.96}$$

$$\tilde{p}_r = p + \alpha p_r^\theta, \tag{2.97}$$

$$\tilde{p}_\perp = p + \alpha p_\perp^\theta. \tag{2.98}$$

Then, following the MGD protocol as in the (3+1) dimensional case, we perform the deformation in the radial part

$$e^{-\lambda(r)} = \mu(r) + \alpha w(r) \tag{2.99}$$

obtaining that our three sectors are given by

1. **Isotropic Sector:** whose line elements is

$$ds^2 = -e^{\nu(r)}dt^2 + \frac{1}{\mu(r)}dr^2 + r^2 d\phi^2, \tag{2.100}$$

and the EFE (2.91) become

$$\kappa^2 \rho = -\Lambda - \frac{\mu'}{2r}, \tag{2.101}$$

$$\kappa^2 p = \Lambda + \frac{\mu\nu'}{2r}, \tag{2.102}$$

$$\kappa^2 p = \Lambda + \frac{\mu'\nu' + \mu\left(2\nu'' + \nu'^2\right)}{4}. \tag{2.103}$$

2. **Decoupler sector** It is worth mentioning that in contrast to the (3+1)-dimensional case, the decoupler sector in (2+1)-dimensional space-time corresponds to the EFE (without cosmological constant) 2.1. Therefore, the line elements for this sector is

$$ds^2 = -e^{\nu(r)}dt^2 + \frac{1}{w(r)}dr^2 + r^2 d\phi^2, \tag{2.104}$$

and the EFE for the source $\theta_{\mu\nu}$ are given by

$$\kappa^2 \rho^\theta = -\frac{w'}{2r}, \tag{2.105}$$

$$\kappa^2 p_r^\theta = \frac{w\nu'}{2r}, \tag{2.106}$$

$$\kappa^2 p_\perp^\theta = \frac{w'\nu' + w\left(2\nu'' + \nu'^2\right)}{4}. \tag{2.107}$$

3. **Total Sector:** The total sector line elements are given by

$$ds^2 = -e^{\nu(r)}dt^2 + \frac{1}{\mu + \alpha w(r)}dr^2 + r^2 d\phi^2, \tag{2.108}$$

and the EFE (2.91) become

$$\kappa^2(\rho + \alpha\rho^\theta) = -\Lambda - \frac{\mu'}{2r} - \alpha\left(\frac{w'}{2r}\right), \tag{2.109}$$

$$\kappa^2(p + \alpha p_r^\theta) = \Lambda + \frac{\mu\nu'}{2r} + \alpha\left(\frac{w\nu'}{2r}\right), \tag{2.110}$$

$$\kappa^2(p + \alpha p_\perp^\theta) = \Lambda + \frac{\mu'\nu' + \mu\left(2\nu'' + \nu'^2\right)}{4} + \alpha\left[\frac{w'\nu' + w\left(2\nu'' + \nu'^2\right)}{4}\right]. \tag{2.111}$$

Therefore, we have again two set of equations. One that corresponds to the perfect fluid (2.101)-(2.103), with the following unknowns $\{\mu,\nu,\rho,p\}$ and a decoupler sector that again only interact gravitationally (2.64), with the following unknowns $\{f,\rho^\theta,p_r^\theta,p_\perp^\theta\}$. Thus, we need to consider a know isotropic solution and a equation of state for $\{\rho^\theta,p_r^\theta,p_\perp^\theta\}$ in order to obtain a new anisotropic solution in (2+1) dimensions [45].

2.2.3 Inverse Minimal Geometric Method in (2+1) Dimensional Gravity

MGD protocol can be seen as an extension of isotropic solutions. In this sense, one can ask if it is possible to start with an anisotropic solution and obtain the isotropic and decoupler source of such a solution. To be more precise, we can wonder which combination of sources $T_{\mu\nu}$ and $\theta_{\mu\nu}$ allows to the formation of a well know anisotropic system. This inverse protocol allows us to shed light about the mechanism behind such anisotropic solutions [16] (Figure 2.8). However, MGD inverse method in (3+1) dimensional gravity gives rise to formal expressions in terms of integrals, which make it difficult to solve them analytically [16]. For that reason, we are going to consider a more simplistic case for a (2+1) dimensional gravity.
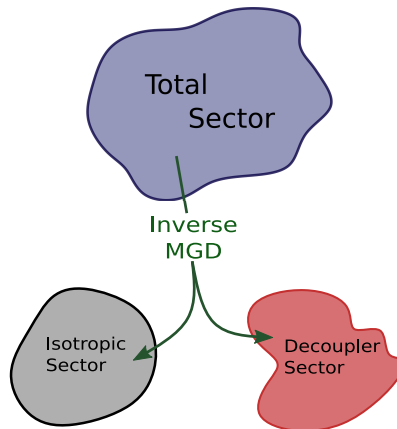

Figure 2.8: Illustration of how from a total anisotropic solution it is obtained the sources through inverse MGD.

In order to apply the inverse method for a (2+1) dimensional gravity, we need to recall the definitions for the effective density and pressures of the total sector (2.96), (2.97) and (2.98). By subtracting (2.97) and (2.98) we obtain the anisotropy

$$\tilde{p}_\perp - \tilde{p}_r = \alpha \left(p_\perp^\theta - p_r^\theta \right). \tag{2.112}$$

Then, we obtain the values of p_r^θ and $p_\perp^\theta$ given by (2.106) and (2.107), respectively. Next, we obtain the values of $\tilde{p}_r$ and $\tilde{p}_\perp$ given by (2.94) and (2.95), respectively. Finally, we replace the values of $\{p_r^\theta, p_\perp^\theta, \tilde{p}_r, \tilde{p}_\perp\}$ in (2.112) obtaining the following differential equation

$$\frac{e^{-\lambda} \left[\nu' \left(r\lambda' + \alpha e^\lambda r w' - 2\alpha e^\lambda w + 2 \right) + 2r\nu'' \left(\alpha e^\lambda w - 1 \right) + r(\nu')^2 \left(\alpha e^\lambda w - 1 \right) \right]}{\kappa r} = 0, \tag{2.113}$$

It is worth mentioning that this can be solved analytically in terms of $w(r)$, contrary to the inverse MGD in (3+1)-dimension that leads to formal expressions for $w(r)$ [16]. The solution in (2+1) dimensional gravity is

$$w(r) = \frac{c_1 r^2 e^{-\nu(r)}}{\nu'(r)^2} + \frac{e^{-\lambda(r)}}{\alpha}, \tag{2.114}$$

where c_1 is a integration constant. Now, let us replace the (2.114) into (2.99) and solve for $\mu(r)$

$$\mu(r) = -\frac{\alpha c_1 r^2 e^{-\nu(r)}}{\nu'(r)^2}. \tag{2.115}$$

Notice that if $c_1 \to 0$ there is not deformation. From these we can obtain the matter content for the isotropic sector,

$$\rho = -\frac{\alpha c_1 e^{-\nu} \left[2r\nu'' + \nu' \left(r\nu' - 2 \right) \right]}{2\kappa^2 (\nu')^3} - \frac{\Lambda}{\kappa^2}, \tag{2.116}$$

$$p = \frac{\Lambda}{\kappa^2} - \frac{\alpha c_1 e^{-\nu} r}{2\kappa^2 \nu'}, \tag{2.117}$$

and for the decoupler sector,

$$\rho^\theta = \frac{c_1 e^{-\nu} \left[2r\nu'' + \nu' \left(r\nu' - 2 \right) \right]}{2\kappa^2 (\nu')^3} + \frac{e^{-\lambda} \lambda'}{\alpha 2\kappa^2 r}, \tag{2.118}$$

$$p_r^\theta = \frac{c_1 e^{-\nu} r}{2\kappa^2 \nu'} + \frac{e^{-\lambda} \nu'}{2\alpha \kappa^2 r}, \tag{2.119}$$

$$p_\perp^\theta = \frac{e^{-\lambda} \left[-\lambda' \nu' + 2\nu'' + (\nu')^2 \right]}{4\alpha \kappa^2} + \frac{2c_1 e^{-\nu} r}{4\kappa^2 \nu'}. \tag{2.120}$$

Thus, given an initial anisotropic solution, the inverse MGD in (2+1)-dimension leads to exact analytical expressions. In contrast to its counterpart in (3+1)-dimension, where it is obtained formal expressions.

2.3 Dualities by Inverse Minimal Geometric Deformation

The inverse MGD problem has been studied in (3+1) and (2+1) dimensions revealing a kind of duality between the topologies and/or sources. To be more precise, it was found in (3+1)-dimensions that, given an AdS polytropic black

hole which is a non-regular solution that satisfies all the energy conditions, the isotropic sector violates the energy conditions after implementing the inverse MGD protocol, giving rise to exotic matter [18]. Similarly, for an initial wormhole solution, which violates the energy conditions, it was obtained that the isotropic and the decoupler sector satisfies all the energy conditions [16]. In the same manner, given a particular regular anisotropic black hole solution with non-linear dynamics satisfying the weak energy condition in (2+1)-dimensions [46], the isotropic sector obtained from the inverse problem leads to either a regular black hole that violates the weak energy condition, or a non-regular black hole that satisfies the weak energy condition [17]. Notice that these examples lead to conclude that may exist a duality between the topologies and/or the sources induced by the inverse MGD. However, the mathematical or physical mechanism whereby this duality happens is still unknown. The main objective of this research project is to study this duality behaviour, focusing on $(2 + 1)$ dimensional models for simplicity. To accomplish this purpose, we are going to present a review of a specific case, and analysis considering a general anisotropic $(2 + 1)$-dimensional case.

Chapter 3

Results & Discussion

In this chapter, we will provide a review of the duality behaviour presented in a (2+1)-dimensional space time. Then, we will propose a mathematical and physical analysis of the duality found in the review, considering a general case. Next, we will present energy and geometric constraints to the seed solution used in the inverse MGD. We will point out the similarity of the energy constraints with the well known BTZ black hole solution[28]. Finally, an explanation to the duality behaviour will be given and we will show that for the solution used in the review it is impossible to obtain regular sources with positive density.

3.1 Duality Review

In this section, we will present a review of the paper[17] with a special emphasis on the dualities found after the application of the inverse MGD.

To start, let us consider a circularly symmetric metric used in[17][46]

$$ds^2 = -f(r)dt^2 + \frac{1}{f(r)}dr^2 + r^2 d\phi^2. \tag{3.1}$$

In this case, $e^{\nu(r)} = f(r)$ and $e^{\lambda(r)} = \frac{1}{f(r)}$. Now, let us consider the total sector as the regular black hole solution for non linear electrodynamics source[46] given by

$$f(r) = -M - \Lambda r^2 - q^2 log(a^2 + r^2), \tag{3.2}$$

where M, Λ, a and q are free parameters. Then, replacing (3.2) in (2.93)-(2.95) we obtain the solutions for the matter content in the total sector

$$\tilde{\rho} = \frac{q^2}{8\pi(a^2 + r^2)}, \tag{3.3}$$

$$\tilde{\rho}_r = -\frac{q^2}{8\pi(a^2 + r^2)}, \tag{3.4}$$

$$\tilde{\rho}_\perp = -\frac{q^2(r^2 - a^2)}{8\pi(a^2 + r^2)^2}, \tag{3.5}$$

and the scalars of curvature obtained from replacing (3.2) in the metric (3.1) are given by

$$R = \frac{2q^2(3a^2 + r^2)}{(a^2 + r^2)^2} + 6\Lambda, \tag{3.6}$$

$$Ricc = \frac{8\Lambda q^2 \left(3a^2 + r^2\right)}{\left(a^2 + r^2\right)^2} + \frac{4q^4 \left(3a^4 + 2a^2 r^2 + r^4\right)}{\left(a^2 + r^2\right)^4} + 12\Lambda^2, \tag{3.7}$$

$$\mathcal{K} = \frac{8\Lambda q^2 \left(a^2 + r^2\right)^2 \left(3a^2 + r^2\right) + 12\Lambda^2 \left(a^2 + r^2\right)^4 + 4q^4 \left(3a^4 + 2a^2 r^2 + r^4\right)}{\left(a^2 + r^2\right)^4}, \tag{3.8}$$

from where it is clear that the scalars are regular in the sense that none of them diverge.

Now, let us apply the MDG inverse problem to obtain the isotropic and the decoupler matter content generators of this regular black hole solution. We need to replace the value of (3.2) in (2.114) and (2.115), respectively, obtaining

$$w(r) = -\frac{c_1(a^2 + r^2)\left[q^2 log(a^2 + r^2) + M + \Lambda r^2\right]}{4\left[\Lambda(a^2 + r^2) + q^2\right]^2} - \frac{q^2 log(a^2 + r^2) + M + \Lambda r^2}{\alpha}, \tag{3.9}$$

$$\mu(r) = \frac{\alpha c_1(a^2 + r^2)^2 \left[q^2 \log (a^2 + r^2) + M + \lambda r^2\right]}{4\left[\Lambda(ar + r^2) + q^2\right]^2}. \tag{3.10}$$

3.1.1   Isotropic Sector

Now, let us focus in the isotropic sector. Replacing (3.9) and (3.10) in (2.116) and (2.117) the information of the matter content for the perfect fluid reads

$$\rho = -\frac{\alpha c_1 a_r^2 \left[2\Lambda q^2(a_r^2 + r^2) + \Lambda^2 a_r^2 + 2Mq^2 + q^4\right]}{32\pi \lambda_r^2} - \frac{2\alpha c_1 q^4 a_r^2 \log a_r^2 + 4\Lambda \lambda_r^3}{32\pi \lambda_r^3}, \tag{3.11}$$

$$p = \frac{\alpha c_1(a^2 + r^2)}{32\pi \left[\Lambda(a^2 + r^2) + q^2\right]} + \frac{\Lambda}{8\pi}, \tag{3.12}$$

where

$$a_r^2 := a^2 + r^2, \tag{3.13}$$

$$\lambda_r := \Lambda a_r^2 + q^2. \tag{3.14}$$

Then, considering the line elements for the isotropic sector

$$ds^2 = -f(r)dt^2 + \frac{1}{\mu(r)}dr^2 + r^2d\phi^2, \tag{3.15}$$

we obtain that the curvature scalars are given by

$$R = -\frac{\alpha c_1\left(a^2 + r^2\right)\left[2q^4\log\left(a^2 + r^2\right) + 2\Lambda q^2\left(3a^2 + 4r^2\right) + 3\Lambda^2\left(a^2 + r^2\right)^2 + 2Mq^2 + 3q^4\right]}{2\lambda_r^3}, \tag{3.16}$$

$$Ricc = \frac{c_1^2 a_r^2\left\{13q^4\left[q^2\log\left(a_r^2\right) + M + \Lambda r^2\right]^2 + 26\left(\Lambda q a_r^2 + q^3\right)^2\left[q^2\log\left(a_r^2\right) + M + \Lambda r^2\right] + 14\lambda_r^4\right\}}{4\lambda_r^6}, \tag{3.17}$$

$$\mathcal{K} = \frac{c_1^2 a_r^2\left\{13q^4\left[q^2\log\left(a_r^2\right) + M + \Lambda r^2\right]^2 + 13\left(\Lambda q a_r^2 + q^3\right)^2\left[q^2\log\left(a_r^2\right) + M + \Lambda r^2\right] + 7\lambda_r^4\right\}}{2\lambda_r^6}. \tag{3.18}$$

The curvature scalars regularity depends on the value of Λ. For $\Lambda > 0$, then $\lambda_r \neq 0$ for any real value of r. However, for $\Lambda < 0$ there exist at least one value that makes that λ_r vanish, which implies that the scalars diverge.

3.1.2 Decoupler sector

Regarding the decoupler sector, we follow the same procedure. Replacing (3.2) in (2.118)-(2.120), we obtain that the matter content for the decoupler sector corresponds to

$$\rho^\theta = \frac{c_1 a_r^2\left[2\Lambda q^2(a_r^2 + r^2) + \Lambda^2 a_r^4 + 2Mq^2 + q^4\right]}{4\lambda_r^3} + \frac{q^2}{\alpha a_r^2} + \frac{c_1 q^4 a_r^2\log a_r^2}{2\lambda_r^3} + \frac{\Lambda}{\alpha}, \tag{3.19}$$

$$p_r^\theta = -\frac{c_1 a_r^2}{4\lambda_r} - \frac{q^2}{\alpha c_r^2} + \frac{\Lambda}{\alpha}, \tag{3.20}$$

$$p_\perp^\theta = \frac{q^2(r^2 - a^2)}{\alpha a_r^4} - \frac{c_1 a_r^2}{a\lambda_r} - \frac{\Lambda}{\alpha}. \tag{3.21}$$

Now, let consider the line element of the decoupler sector to study the geometry of this sector

$$ds^2 = -f(r)dt^2 + \frac{1}{w(r)}dr^2 + r^2d\phi^2, \tag{3.22}$$

replacing (3.9) in (3.22) we obtain taht for a $\Lambda > 0$ the event horizon for this solution could be obtained by solving

$$-M - \Lambda r^2 - q^2\log(a^2 + r^2) = 0.$$

Then, the scalars of curvature are given by

$$R = \frac{\mathcal{H}_1}{2\alpha(a^2 + r^2)^2\left(\Lambda(a^2 + r^2) + q^2\right)^3}, \tag{3.23}$$

$$Ricc = \frac{\mathcal{H}_2}{36(a^2 + r^2)^4\left(\Lambda(a^2 + r^2) + q^2\right)^6}, \tag{3.24}$$

$$\mathcal{K} = \frac{\mathcal{H}_3}{36(a^2 + r^2)^4\left(\Lambda(a^2 + r^2) + q^2\right)^6}. \tag{3.25}$$

where $\mathcal{H}_1$, $\mathcal{H}_2$ and $\mathcal{H}_3$ are long functions in terms of polynomials of r and $\log(a^2 + r^2)$. The regularity of this sector also depends on the sing of Λ. For $\Lambda < 0$, we obtain a non-regular black hole solution. Whereas, for $\Lambda > 0$, we have a regular black hole solution.

3.1.3 Energy Conditions

Now let us summarize the results obtained in reference 17 with respect to the energy conditions and illustrate the conjectured duality behaviour proposed by the author.

First, we are going to consider $\Lambda > 0$. In this case both sectors isotropic and decoupler correspond to regular black hole solutions, with horizon at $-M - \Lambda r_H - q^2 \log(a^2 + r^2) = 0$. Unfortunately, due to the nature of the solution we should consider numerical analysis of the solutions. For this subsection we are going to fix the following values for the constants: $\Lambda = 2, M = 1, q = 1$ and $a = 0.1$.

Isotropic Sector, $\Lambda > 0$

For the isotropic sector we evaluate the value of ρ for different values of αc_1 (Figure. 3.1).
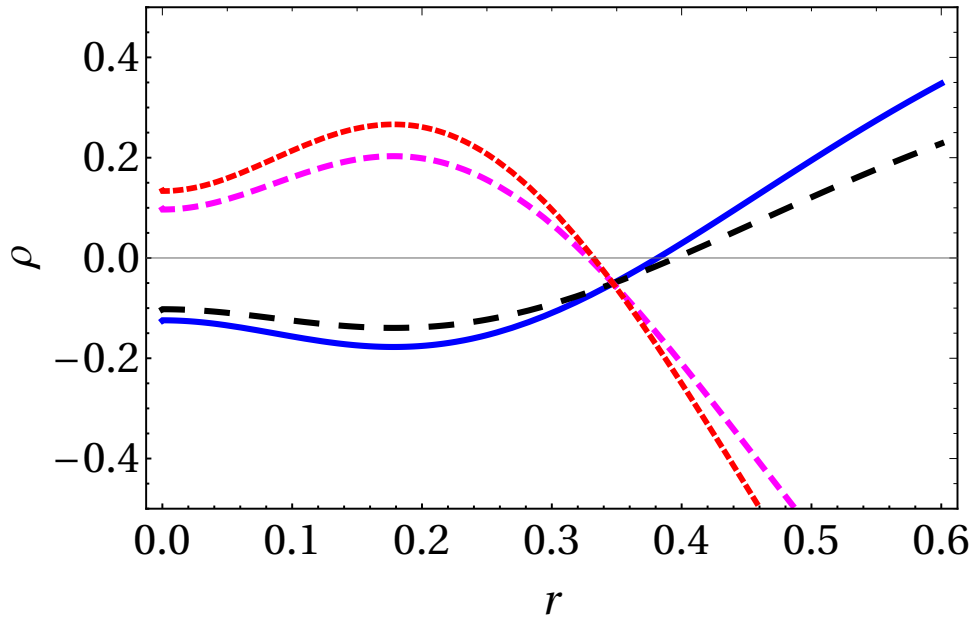

Figure 3.1: Energy density plot for the isotropic sector. (Blue line) $\alpha c_1 = -200$. (Black dashed line) $\alpha c_1 = -140$. (Magenta dashed line) $\alpha c_1 = 400$, (Red dashed line) $\alpha c_1 = 500$

Notice that the density does not remain positive for all the values of r, which implies that the WEC (2.13) is violated unavoidably.

Decoupler sector, $\Lambda > 0$

Regarding the decoupler sector it was found that, there exist certain values of c_1 given by $c_1 \leq \frac{7017.49}{\alpha}$, that allow us to eliminate the apparition of $\rho \leq 0$ (exotic matter). In particular, if we fix the value of $\alpha = 1$ it can be observed that the density in the decoupler sector remain positive for all the values of r (Figure 3.2).

Figure 3.2: Energy density plot for the decoupler sector. (Blue line) $c_1 = 1$. (Black dashed line) $c_1 = 10$. (Magenta dashed line) $c_1 = 50$, (Red dashed line) $c_1 = 100$

These two numerical results suggest that for positive values of Λ it is impossible to avoid the exotic matter for the isotropic and decoupler sectors, simultaneously.

On the other hand, for $\Lambda < 0$ we fix the following values for the constants: $M = 2$, $q = 1$, $a = 1$ and $\Lambda = -0.902359\,^{17}$ because $r_H^2 + a^2 < 1$ and $q^2|\log(a^2 + r_H^2)| > M$ or $r^2 + a^2 > 1$. For these values the horizon is located at $r_H = 2$ and the singularity at $r_c = 0.328946$. Thus, this solution corresponds to an irregular black hole solution. It is important to remark that we need to consider only positive values for αc_1 for both sectors in order to avoid exotic matter.

Isotropic Sector, $\Lambda < 0$

For the Isotropic sector it was found that for different values of $\alpha c_1 > 0$ it is possible to obtain positive values of the density as it is observed in the Figure. 3.3.

Figure 3.3: Energy density plot for the isotropic sector. (Blue line) $\alpha c_1 = 0.1$. (Black dashed line) $\alpha c_1 = 0.2$. (Magenta dashed line) $\alpha c_1 = 0.5$, (Red dashed line) $\alpha c_1 = 1$

Decoupler Sector, $\Lambda < 0$

For the decoupler sector we are going to consider negative values for α and c_1. For simplicity, we fix the value of $\alpha = -1$. Observe that in this sector, as in the previous one $\rho^\theta \geq 0$ (Figure. 3.4).

This results for negative values of Λ suggest that it is possible to avoid negative values of density for the isotropic and decoupler sectors. Unfortunately, negative values of Λ implies that the solutions correspond to non-regular black holes as it is pointed out by Contreras[17].

Finally, the behaviour of the solutions presented in this review is summarized in the table 3.1. From these results it is importat to remark two main aspects. First, the duality between positive density and regularity of the solutions depend on the choice of Λ. Second, the duality behaviour is focalized in the isotropic sector.

Λ	Regularity		$\rho \geq 0$	
	Isotropic	Decoupler	Isotropic	Decoupler
> 0	✓	✓	x	✓
< 0	x	x	✓	✓

Table 3.1: behaviour of the solutions obtained using MGD inverse method in the isotropic and decoupler sector in dependence of the values of Λ.
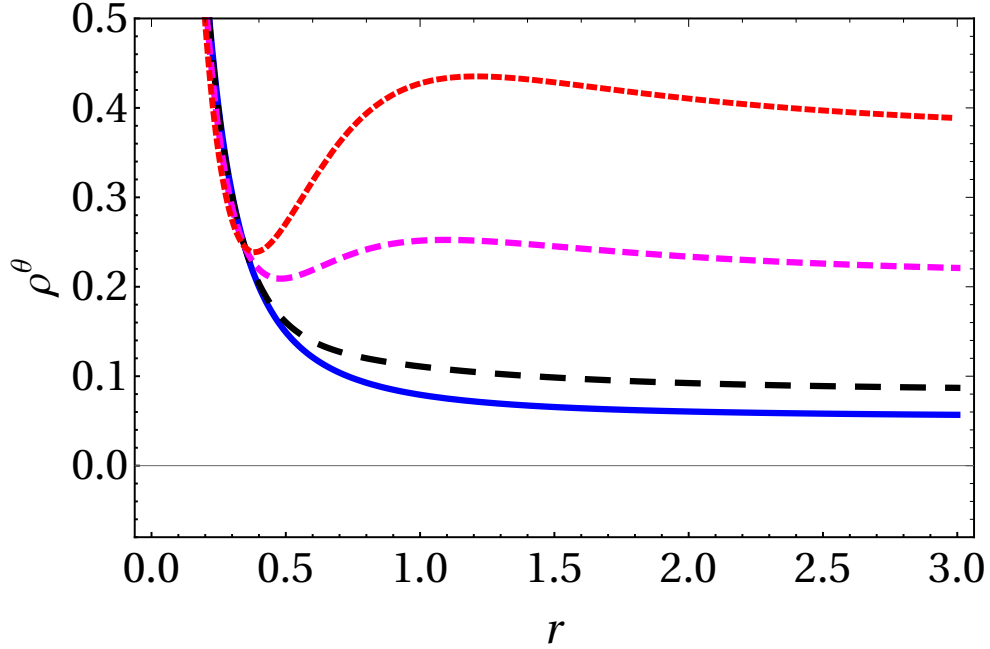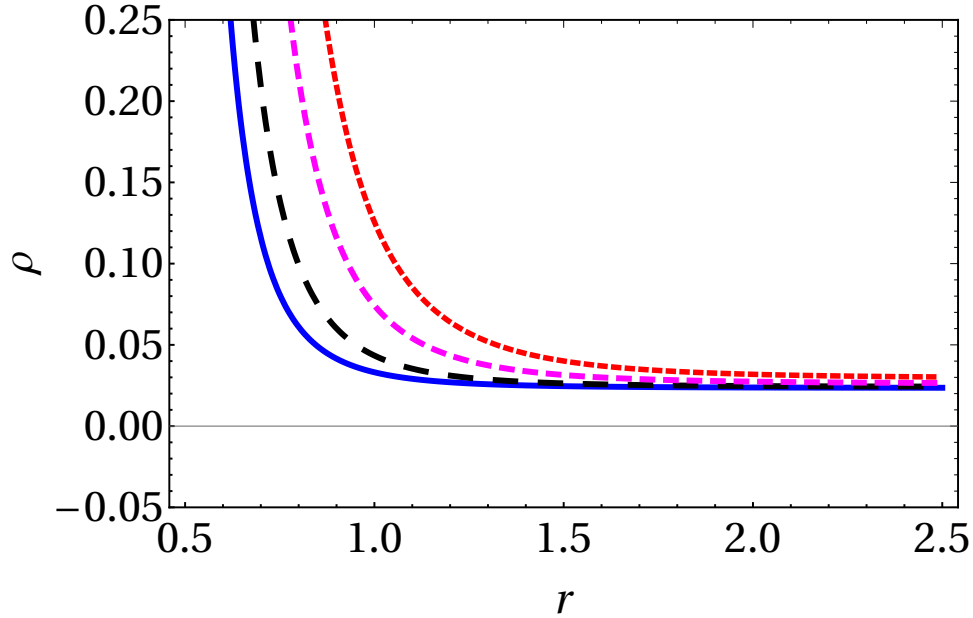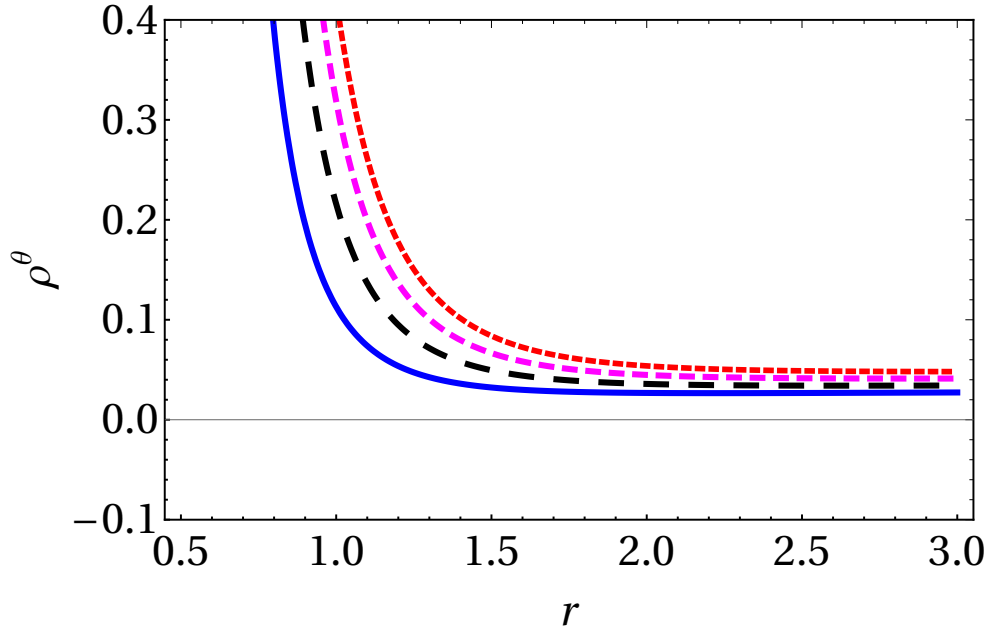
Figure 3.4: Energy density plot for the isotropic sector. (Blue line) $c_1 = -1$. (Black dashed line) $c_1 = -2$. (Magenta dashed line) $c_1 = -3$, (Red dashed line) $c_1 = -4$

3.2 Duality

In this section, a mathematical treatment to the duality found in section 3.1, based on simple physical and mathematical assumptions, will be provided. First, we will obtain constraints for the seed solution used in the inverse MGD to avoid the violation of $\rho \geq 0$ for all the sectors. Next, the geometrical problems with the curvature scalars will be studied. Finally, weak complementary constraints to avoid the non-regularity of the solutions in all the sectors will be presented.

3.2.1 Energy Constraints

In this subsection, we will study the matter content of the three sectors obtained by the inverse MGD. We will ensure $\rho \geq 0$ in all the sectors to avoid exotic matter. For all the computations in this subsection We will consider that $e^{\nu(r)} = f(r)$ and $e^{\lambda(r)} = \frac{1}{f(r)}$ in (2.92).

Total Sector

First, let us consider the line elements of the total sector, which corresponds to the seed solution of the inverse MGD (2.92),

$$ds^2 = -f(r)dt^2 + \frac{1}{f(r)}dr^2 + r^2 d\phi^2, \tag{3.26}$$

from this we can compute the energy density for the sector

$$\tilde{\rho}(r) = -\frac{2\Lambda r + f'(r)}{2r\kappa}. \tag{3.27}$$

To satisfy $\rho \geq 0$, the equation (3.27) need to be greater or equal than zero, which implies that

$$f'(r) \leq -2r\Lambda, \tag{3.28}$$

after integrating with respect to r, we obtain

$$f(r) \leq -r^2\Lambda + q_1, \tag{3.29}$$

where q_1 is a constant of integration. Notice that this condition is only valid to satisfy the energy conditions in the total sector.

Isotropic Sector

The line element of the isotropic sector is given by (2.100)

$$ds^2 = -f(r)dt^2 + \frac{1}{\mu(r)}dr^2 + r^2 d\phi^2, \tag{3.30}$$

where $\mu(r)$ will be expressed as $\mu(r) = f(r)g(r)$, with $g(r) = -\frac{c_1 r^2 \alpha}{f'(r)^2}$. To be more precise, μ can corresponds to

$$\mu(r) = -\frac{\alpha c_1 r^2 f(r)}{f'(r)^2}, \tag{3.31}$$

where c_1 is a constant of integration and α corresponds to the parameter of the MGD (Section 2.2.2). It is important to remark that in order to preserve the event horizon in the isotropic and total sector, we should impose that $g(r)$ does not vanish at the same values as $f(r)$ vanish. Moreover, to avoid that $g(r)$ diverge we should impose that $f'(r) \neq 0$.

Next, we obtain the energy density for this sector,

$$\rho = -\frac{2r\Lambda + (f(r)g(r))'}{2r\kappa^2}. \tag{3.32}$$

Note that to ensure $\rho \geq 0$, we should satisfy the following differential inequality

$$(f(r)g(r))' \leq -2r\Lambda, \tag{3.33}$$

which after integration results in

$$f(r)g(r) \leq -r^2\Lambda + q_2, \tag{3.34}$$

where q_2 is a constant of integration.

Decoupler Sector

The metric function for the decoupler sector is given by

$$w(r) = \frac{c_1 r^2 f(r)}{f'(r)^2} + \frac{f(r)}{\alpha}. \tag{3.35}$$

Next, we consider the decoupler sector line elements (2.104), given by

$$ds^2 = -f(r)dt^2 + \frac{1}{w(r)}dr^2 + r^2 d\phi^2, \tag{3.36}$$

where $w(r)$ si given by (3.35). From this we can compute the energy density of this sector

$$\rho^\theta = \frac{-f'(r) + (f(r)g(r))'}{2r\kappa^2}. \tag{3.37}$$

To satisfy $\rho^\theta \geq 0$ we need to satisfy the differential inequality

$$f'(r) \leq (f(r)g(r))', \tag{3.38}$$

from where, after integration, we obtain

$$f(r) \leq f(r)g(r) + q_3, \tag{3.39}$$

where q_3 is a constant of integration.

Constraints

As we mention before, we require that all the sectors satisfy $\rho \geq 0$ simultaneously to avoid the presence of exotic matter in the solutions. In order to solve this problem we should solve a system of inequalities obtained from (3.28), (3.33) and (3.38).

$$\mathcal{S}_1 \begin{cases} f'(r) \leq -2r\Lambda, & \text{(3.28) Total Sector} \\ (f(r)g(r))' \leq -2r\Lambda, & \text{(3.33) Isotropic Sector} \\ f'(r) \leq (f(r)g(r))', & \text{(3.38) Decoupler Sector} \end{cases} \tag{3.40}$$

which after integration leads to other system of inequalities

$$\mathcal{S}_2 = \begin{cases} f(r) \leq -r^2\Lambda + q_1, & \text{(3.29) Total Sector} \\ f(r)g(r) \leq -r^2\Lambda + q_2, & \text{(3.34) Isotropic Sector} \\ f(r) \leq f(r)g(r) + q_3. & \text{(3.39) Decoupler Sector} \end{cases} \tag{3.41}$$

Notice that the system $\mathcal{S}_1$ can be summarized in the following differential inequality,

$$f'(r) \leq (f(r)g(r))' \leq -2r\Lambda. \tag{3.42}$$

Next, let us consider the system $\mathcal{S}_2$, if we sum the constant q_3 to both sides of (3.34), we obtain

$$f(r)g(r) + q_3 \leq -r^2\Lambda + q_2 + q_3. \tag{3.43}$$

Note that, if we compare (3.43) with (3.39), we obtain

$$f(r) \leq f(r)g(r) + q_3 \leq -r^2\Lambda + q_2 + q_3. \tag{3.44}$$

After that, we fix the value of q_1 as $q_1 = q_2 + q_3$, from where we obtain

$$f(r) \leq f(r)g(r) + q_3 \leq -r^2\Lambda + q_1. \tag{3.45}$$

For simplicity we can assume $q_3 = 0$, due to the main inequality that we need to satisfy is (3.42). Therefore, we can simplify (3.45) as

$$f(r) \leq f(r)g(r) \leq -r^2\Lambda + q_1, \tag{3.46}$$

considering that $g(r) = -\frac{\alpha c_1 r^2}{f'(r)^2}$, we obtain

$$f(r) \leq -f(r)\frac{\alpha c_1 r^2}{f'(r)^2} \leq -r^2\Lambda + q_1. \tag{3.47}$$

Given that $r^2, f'(r)^2 > 0$, this implies that $\alpha c_1 < 0$, necessarily. Moreover, we need that the derivative of $f'(r)$ do not vanish for any value of r to ensure the inequality.

Thus, we conclude with the following set of constraints to $f(r), f'(r)$ and the constants α, c_1 to ensure that $\rho \geq 0$ in all the sectors,

Energy Constraints (Integrated expressions version):

$$f(r) \leq -r^2\Lambda + q_1 \tag{3.48}$$

$$f(r) \leq -f(r)\frac{\alpha c_1 r^2}{f'(r)^2} \leq -r^2\Lambda + q1, \tag{3.49}$$

$$f'(r) \neq 0, \tag{3.50}$$

$$c_1\alpha < 0. \tag{3.51}$$

Energy Constraints (original expressions version):

$$f'(r) \leq -2r\Lambda, \tag{3.52}$$

$$(f(r)g(r))' \leq -2r\Lambda, \tag{3.53}$$

$$f'(r) \leq (f(r)g(r))' \tag{3.54}$$

$$f'(r) \neq 0, \tag{3.55}$$

$$c_1\alpha < 0. \tag{3.56}$$

It is worth mentioning that the integrated expressions of the energy constraints allow to an easier computation and verification. However, the unknown constants q_1, q_2, q_3 could lead to inconclusive results due to the freedom of choice.

Upper bound to Energy Constraints

It is important to mention that (3.48) is similar to the vacuum BTZ black hole solution (2.54)[28]. This could mean that BTZ black hole solution is an upper bound of $f(r)$. To illustrate this, let us consider

$$f(r) = -r^2\Lambda + q_1 \tag{3.57}$$

, which corresponds to a general form of the BTZ vacuum solution 2.56, and let us replace it in (3.49)

$$-r^2\Lambda + q_1 \leq -r^2\Lambda + q_1\left(-\frac{\alpha c_1}{4\Lambda^2}\right) \leq -r^2\Lambda + q_1. \tag{3.58}$$

This could only correspond to the saturated solution of the inequalities (3.49),

$$-r^2\Lambda + q_1 = -r^2\Lambda + q_1\left(-\frac{\alpha c_1}{4\Lambda^2}\right) = -r^2\Lambda + q_1, \tag{3.59}$$

which implies that $-\frac{\alpha c_1}{4\Lambda^2} = 1$. In this sense, we obtain a condition to the cosmological constant Λ of BTZ solution under inverse MGD,

$$-\sqrt{-\frac{\alpha c_1}{4}} = \Lambda = \sqrt{-\frac{\alpha c_1}{4}}, \tag{3.60}$$

for $\alpha c_1 < 0$. This show that BTZ solution (2.56), for $\Lambda = -\frac{1}{\ell^2}$, corresponds to a solution of the saturated inequality (3.49). This suggest that (2.56) can be consider as an upper limit for the conditions (3.49). We will return to this argument later.

3.2.2 Geometric Constraints

In this subsection, we will study the regularity of the curvature scalars under inverse MGD, on the three sectors. We will present some weak conditions to avoid the non-regularity of the scalars in the three sectors. It is important to clarify that by non-regularity we mean non-divergent behaviour of the curvature scalars. For simplicity, we will omit long expressions in the numerator and we only will focus on the expression in the denominator, which are the ones that give rise to the divergent behaviour of the scalars. The scalars that we are going to consider for this study of the regularity will be Ricci Scalar (2.3)

$$R = g^{\mu\nu}R_{\mu\nu}, \tag{3.61}$$

Ricci Square

$$\mathcal{R}cc = R_{\alpha\beta}R^{\alpha\beta}, \tag{3.62}$$

and Kretschmann scalar (2.48)

$$\mathcal{K} = R_{\alpha\beta\sigma\gamma}R^{\alpha\beta\sigma\gamma}. \tag{3.63}$$

Total Sector

First, let us consider the line elements that corresponds to the total sector (3.26),

$$ds^2 = -f(r)dt^2 + \frac{1}{f(r)}dr^2 + r^2 d\phi^2, \tag{3.64}$$

from this we can obtain the curvature invariants

- **Ricci Scalar:**

$$R_{tot} = -f''(r) - \frac{2f'(r)}{r}. \tag{3.65}$$

- **Ricci Square:**

$$\mathcal{R}cc_{tot} = \frac{2f'(r)^2 + [rf''(r) + f'(r)]^2}{2r^2}. \tag{3.66}$$

- **Kretschmann Scalar:**

$$\mathcal{K}_{tot} = f''(r)^2 + \frac{2f'(r)^2}{r^2}. \tag{3.67}$$

At this point, some comments are in order. First, we require that the function $f(r)$ should be at least two times derivable. Second, for the total sector, we only need to verify the limit of the scalars when $r \to 0$ exist and are constant.

Isotropic Sector

Now, let us consider the istropic sector line elements (3.30),

$$ds^2 = -f(r)dt^2 + \frac{1}{\mu(r)}dr^2 + r^2 d\phi^2, \tag{3.68}$$

the computed curvature scalars read as

- **Ricci Scalar:**

$$R_{iso} = \frac{\alpha c_1 \left\{ 3rf'(r)^2 + 2f(r)\left[f'(r) - rf''(r)\right]\right\}}{f'(r)^3}. \tag{3.69}$$

- **Ricci Square:**

$$\mathcal{R}cc_{iso} = \frac{c_1^2 \left\{ 14r^2 f'(r)^4 + 26rf(r)f'(r)^2 \left[f'(r) - rf''(r)\right] + 13f(r)^2 \left[f'(r) - rf''(r)\right]^2\right\}}{f'(r)^6}. \tag{3.70}$$

- **Kretschmann Scalar:**

$$\mathcal{K}_{iso} = \frac{2c_1^2 \left\{ 7r^2 f'(r)^4 + 13rf(r)f'(r)^2 \left[f'(r) - rf''(r)\right] + 13f(r)^2 \left[f'(r) - rf''(r)\right]^2\right\}}{f'(r)^6}. \tag{3.71}$$

Notice that if the derivative of $f(r)$ vanish for some point in the reals, the scalars could present a divergent behaviour when r approaches to the roots of $f'(r)$. Therefore, as a weak condition, we could verify that the limit for all the curvature scalars when $r \to \tilde{r}$, where $\tilde{r}$ is a root of $f'(r)$, exist and are constants. Moreover, we can observe that these curvature scalars do not have a specific problem when $r \to 0$ unless it is a root of $f'(r)$.

Decoupler Sector

Finally, we will consider the line elements for the decoupler sector (3.36),

$$ds^2 = -f(r)dt^2 + \frac{1}{w(r)}dr^2 + r^2 d\phi^2, \tag{3.72}$$

where, $w(r)$ is defined from the inverse MGD problem as

$$w(r) = \frac{f(r) - f(r)g(r)}{\alpha}. \tag{3.73}$$

Then, the curvature scalars are given by

- **Ricci Scalar:**

$$R_{cou} = -\frac{3c_1 r}{f'(r)} - \frac{2c_1 f(r)\left[f'(r) - rf''(r)\right]}{f'(r)^3} - \frac{f''(r)}{\alpha} - \frac{2f'(r)}{\alpha r} \tag{3.74}$$

- **Ricci Squared:**

$$\mathcal{R}cc_{cou} = \frac{\mathfrak{P}_1}{144r^2 f'(r)^6}, \tag{3.75}$$

- **Kretschmann Scalar:**

$$\mathcal{K}_{cou} = \frac{\mathfrak{P}_2}{72r^2 f'(r)^6}, \tag{3.76}$$

where $\mathfrak{P}_1$ and $\mathfrak{P}_2$ are too long expression that contain polynomial expressions in terms of $f(r)$, $f'(r)$. $f''(r)$ and $f'''(r)$. It is important to remark that from previous expression we should impose that our function $f(r)$ is at least three times derivable. Regarding the divergent behaviour of the scalars, in this case we should ensure that the limit of the scalars for all the sectors when $r \to 0$ and $r \to \tilde{r}$, exist and are constants, where $\tilde{r}$ is a real root of $f'(r)$.

It is important to remark that if $f'(r)$ does not have real roots, we should only verify that the limit when $r \to 0$ for the scalars of total and decoupler sector exist. Otherwise, it should also require to verify that the limit when $r \to \tilde{r}$, where $\tilde{r}$ is a real root of $f'(r)$, for the scalars of the isotropic and decoupler sector exist. From this analysis, we conclude that the regularity on the geometry for inverse MGD depends not only on r but also on the roots of the derivative of $f(r)$. Therefore, we conclude with weak constraints to $f(r)$ to ensure the regularity of the solutions are summarized as follows

Geometrical Constraints:

1. Geometrical Constraint 1:

$$\lim_{r \to 0} R = \alpha, \quad \lim_{r \to 0} \mathcal{R}cc = \beta, \quad \lim_{r \to 0} \mathcal{K} = \gamma \quad \text{(for all the three sectors)} \tag{3.77}$$

   where α, β and γ are real constants.

2. Geometrical Constraint 2:

$$\forall \tilde{r} : \quad f'(\tilde{r}) = 0, \quad \tilde{r} \in i\mathbb{R} \tag{3.78}$$

$$\text{or}$$

$$\exists \tilde{r} \in \mathbb{R}: \quad f'(\tilde{r}) = 0, \Rightarrow \lim_{r \to \tilde{r}} R = \alpha, \quad \lim_{r \to \tilde{r}} \mathcal{R}cc = \beta, \quad \lim_{r \to \tilde{r}} \mathcal{K} = \gamma \text{ (for all the three sectors)} \tag{3.79}$$

where α, β and γ are real constant.

These constraints are considered weak because it requires to compute the limit of the scalars for some values and it does not provide any mathematical either physical explanation to ensure the regularity of the solutions on the three sectors.

3.3 Analysis of the Duality Solution

In this section, the solution used in section 3.1 will be studied under the constraints obtained in the previous section. For the energy constraints, we will consider the BTZ solution as an upper bound as it was discussed in subsection 3.2.1. Later, we will study the implications of our constraints and an explanation of the duality behaviour of the solution will be given. Finally, we will show that the solution used in section 3.1 cannot satisfy the energy and regularity condition for any sector.

3.3.1 Density Analysis

Recall the $f(r)$ used in the section 3.1 is

$$f(r) = -M - \Lambda r^2 - q^2 \log(a^2 + r^2), \quad r \in \mathbb{R}^+ \tag{3.80}$$

whose derivative is

$$f'(r) = -2\Lambda r - \frac{2q^2 r}{a^2 + r^2}. \tag{3.81}$$

Let us start our discussion in terms of the sign of Λ. It is worth mentioning that for negative values of Λ there exist at least one $r_0 \in \mathbb{R}$ such that $f'(r_0) = 0$, which violated constraint (3.55) and made $g(r)$ diverge. In this sense, we will focus our analysis for positive values of Λ. Moreover, we will assume only positive values of M, q and a for all the computations.

First, replacing (3.80) into (3.52), which correspond to the total sector, we obtain

$$f'(r) = -2\Lambda r - \frac{2q^2 r}{a^2 + r^2} \le -2\Lambda r, \tag{3.82}$$

$$\Rightarrow -\frac{2q^2 r}{a^2 + r^2} \le 0, \tag{3.83}$$

this inequality is satisfied for any value of Λ, q, a and r. Therefore, we do not have any problem in the total sector.

Now, let us focus our attention to the isotropic and decoupler sector by replacing equation (3.80) in (3.53) and (3.54), respectively. We obtain:

$$\frac{\alpha c_1 r \left(a^2 + r^2\right)}{2 \left(\Lambda \left(a^2 + r^2\right) + q^2\right)^3} \left[2q^4 \log\left(a^2 + r^2\right) + 2\Lambda q^2 \left(a^2 + 2r^2\right) + \Lambda^2 \left(a^2 + r^2\right)^2 + 2Mq^2 + q^4\right] \leq -2\Lambda r, \tag{3.84}$$

$$\frac{\alpha c_1 r \left(a^2 + r^2\right)}{2 \left(\Lambda \left(a^2 + r^2\right) + q^2\right)^3} \left[2q^4 \log\left(a^2 + r^2\right) + 2\Lambda q^2 \left(a^2 + 2r^2\right) + \Lambda^2 \left(a^2 + r^2\right)^2 + 2Mq^2 + q^4\right] \geq -\frac{2q^2 r}{a^2 + r^2} - 2r\Lambda. \tag{3.85}$$

These two equations can be rewritten as

$$\frac{\alpha c_1 \left(a^2 + r^2\right)}{4\Lambda \left(\Lambda \left(a^2 + r^2\right) + q^2\right)^3} \Xi(r) \leq -1, \tag{3.86}$$

$$\frac{\alpha c_1 \left(a^2 + r^2\right)^2}{4 \left(\Lambda \left(a^2 + r^2\right) + q^2\right)^4} \Xi(r) \geq -1, \tag{3.87}$$

where

$$\Xi(r) = \left[2q^4 \log\left(a^2 + r^2\right) + 2\Lambda q^2 \left(a^2 + 2r^2\right) + \Lambda^2 \left(a^2 + r^2\right)^2 + 2Mq^2 + q^4\right]. \tag{3.88}$$

At this point, it is necessary to make some comments. First, under our assumptions $M > 0$, $\Lambda > 0$ and $q > 0$ the constraint (3.56) becomes a necessary condition to satisfy (3.86) because all the terms correspond to positive values except for $\log(a^2 + r^2)$. This is negative for values of a between zero and one but it does not represent any difficulty in our analysis because the logarithm grows slower than polynomial expressions. Second, even when (3.56) is a necessary condition to satisfy (3.86), for (3.87) this is not true anymore. Finally, the complexity of the expressions force us to study the behaviour of the inequalities in the asymptotics of the expressions.

Let us start our analysis by considering the saturated case for (3.86) and (3.87),

$$\frac{\alpha c_1 \left(a^2 + r^2\right)}{4\Lambda \left(\Lambda \left(a^2 + r^2\right) + q^2\right)^3} \Xi(r) = -1, \tag{3.89}$$

$$\frac{\alpha c_1 \left(a^2 + r^2\right)^2}{4 \left(\Lambda \left(a^2 + r^2\right) + q^2\right)^4} \Xi(r) = -1. \tag{3.90}$$

These equations implies that

$$\frac{\alpha c_1 \left(a^2 + r^2\right)}{4\Lambda \left(\Lambda \left(a^2 + r^2\right) + q^2\right)^3} \Xi(r) = \frac{\alpha c_1 \left(a^2 + r^2\right)^2}{4 \left(\Lambda \left(a^2 + r^2\right) + q^2\right)^4} \Xi(r), \tag{3.91}$$

from this, we obtain

$$\frac{1}{\Lambda} = \frac{\left(a^2 + r^2\right)}{\Lambda(a^2 + r^2) + q^2} \tag{3.92}$$

that, clearly, can only be satisfied if $q = 0$. However, in that case, (3.80) will become

$$f(r) = -M - \Lambda r^2, \tag{3.93}$$

which have the form of a BTZ solution just like equation (3.57) and, at the same time, satisfies positive density for all the sectors (subsection (3.2.1)), and it is not a case of interest. Therefore, we will focus our attention only on the strict inequalities, namely:

$$\frac{\alpha c_1 \left(a^2 + r^2\right)}{4\Lambda \left(\Lambda \left(a^2 + r^2\right) + q^2\right)^3} \Xi(r) < -1, \tag{3.94}$$

$$\frac{\alpha c_1 \left(a^2 + r^2\right)^2}{4 \left(\Lambda \left(a^2 + r^2\right) + q^2\right)^4} \Xi(r) > -1. \tag{3.95}$$

As we mentioned before due to the high complexity of (3.94) and (3.95), we will focus our analysis on the asymptotics of the functions. In particular, we will consider the limit when $r \to \infty$ because both equations are bounded and we should verify if the expressions converge to values that satisfy these bounds. In this sense, the limit when $r \to \infty$ for (3.94) and (3.95) read as

$$\frac{\alpha c_1}{4\Lambda^2} < -1, \tag{3.96}$$

$$\frac{\alpha c_1}{4\Lambda^2} > -1, \tag{3.97}$$

respectively. From these two expressions, we arrived to a contradiction that implies that it is impossible to obtain positive density for both sectors, which explain the behaviour of the table 3.1 exposed in the section (3.1). Finally, we can conclude that for (3.80), under our assumptions and constraints (i.e,f $M > 0$, $q > 0$, $a > 0$, $\alpha c_1 < 0$, $\Lambda > 0$), it is impossible to satisfy the energy conditions for the isotropic and decoupler sector under inverse MGD.

It is important to highlight two aspects from this analysis. First, under the assumptions considered in this section the seed solution (i.e, (3.80)) do not correspond to a black hole solution because $f(r)$ has not real root. Second, even when it can the logarithm can take negative values for $a \in [0, 1]$, the asymptotic behaviour to infinity remains the same and the result is still strong enough.

3.3.2 Geometric Analysis

In this section, we will study the implications of the geometric conditions, (3.77) - (3.79), on the solution (3.2) presented in the section 3.1. We will explain the violation of the regularity of the curvature scalars for certain values of Λ and its relation with our proposed constraints.

3.3.3 Limit $r \to 0$

First, we need to recall the scalars of curvature (3.74), (3.75) and (3.76) for the solution (3.2) (Section (3.1)) and let us study the limit of the scalar when $r \to 0$ (3.77).

Isotropic Sector

Let us recall the isotropic metric (3.30),

$$ds^2 = -f(r)dt^2 + \frac{1}{\mu(r)}dr^2 + r^2d\phi^2,$$

where $\mu(r)$ for the inverse MGD is given by (3.31). In this way, the limit of the curvature scalars for $r \rightarrow 0$ reads

$$\lim_{r \rightarrow 0} R_{iso} = \frac{a^2\alpha \left[ ]3a^4\Lambda^2 + 2q^4 \log\left(a^2\right) + 6a^2\Lambda q^2 + 2Mq^2 + 3q^4 \right]}{2 \left(a^2\Lambda + q^2\right)^3}, \tag{3.98}$$

$$\lim_{r \rightarrow 0} \mathcal{R}cc_{iso} = \frac{\mathfrak{J}_1}{4 \left(a^2\Lambda + q^2\right)^6}, \tag{3.99}$$

$$\lim_{r \rightarrow 0} \mathcal{K}_{iso} = \frac{\mathfrak{J}_2}{2 \left(a^2\Lambda + q^2\right)^6}, \tag{3.100}$$

where $\mathfrak{J}_1$ and $\mathfrak{J}_2$ are expressions which are not relevant for our study of regularity. The limits shows that the curvature scalars have problems for values of $\Lambda = -\frac{q^2}{a^2}$. In the section 3.1 it is used $\Lambda = -2 \neq -\frac{1}{0.1^2}$. This explain the non-divergent behaviour observed in the section 3.1.

Decoupler Sector

Regarding the decoupler sector, the line elements is given by (3.36)

$$ds^2 = -f(r)dt^2 + \frac{1}{w(r)}dr^2 + r^2d\phi^2,$$

where $w(r)$ is given by the inverse MGD (3.35). In this way, the limit of the curvature scalars for $r \rightarrow 0$ reads

$$\lim_{r \rightarrow 0} R_{coup} = \frac{\mathfrak{J}_3}{2a^2\alpha \left(a^2\Lambda + q^2\right)^3}. \tag{3.101}$$

$$\lim_{r \rightarrow 0} \mathcal{R}cc_{coup} = \frac{\mathfrak{J}_4}{36a^4 \left(a^2\Lambda + q^2\right)^6}. \tag{3.102}$$

$$\lim_{r \rightarrow 0} \mathcal{K}_{coup} = \frac{\mathfrak{J}_5}{36a^4 \left(a^2\Lambda + q^2\right)^6}, \tag{3.103}$$

where $\mathfrak{J}_3$, $\mathfrak{J}_4$ and $\mathfrak{J}_5$ are expressions, which are not relevant for our study of regularity. From these expressions we can observe that again the curvature scalars have problems for values of $\Lambda = -\frac{q^2}{a^2}$, which have no problems for the values used in the section 3.1.

Total Sector

Next, the total sector line elements are given by (3.26)

$$ds^2 = -f(r)dt^2 + \frac{1}{f(r)}dr^2 + r^2d\phi^2,$$

the limit of the curvature scalars for $r \rightarrow 0$ reads

$$\lim_{r \to 0} R_{tot} = \frac{6a^4 \Lambda + 6a^2 q^2}{a^4}, \tag{3.104}$$

$$\lim_{r \to 0} \mathcal{R}cc_{tot} = \frac{12a^8 \Lambda^2 + 24a^6 \Lambda q^2 + 12a^4 q^4}{a^8}, \tag{3.105}$$

$$\lim_{r \to 0} \mathcal{K}_{tot} = \frac{12a^8 \Lambda^2 + 24a^6 \Lambda q^2 + 12a^4 q^4}{a^8}. \tag{3.106}$$

The total sector has no divergence in the limit when $r \to 0$.

3.3.4   Limit $r \to \tilde{r}$

Now, let us check the limit when $r \to \tilde{r}$, where $\tilde{r}$ correspond to the roots of $f'(r)$. We should verify that (3.78) is satisfied or (3.79) is satisfied. In this case, the roots of $f'(r)$ are given by

$$f'(\tilde{r}) = -\frac{2q^2 \tilde{r}}{a^2 + \tilde{r}^2} - 2\Lambda \tilde{r} = 0, \tag{3.107}$$

from where is clear that there are three roots. The first one,

$$\tilde{r}_1 = 0, \tag{3.108}$$

which correspond to the previous studied limits $r \to 0$, and

$$\tilde{r}_2 = \sqrt{\frac{-q^2 - a^2 \Lambda}{\Lambda}}. \tag{3.109}$$

The last two roots can be either pure imaginary or real, depending on the sign of Λ. For $\Lambda < 0$ the roots are reals and for $\Lambda > 0$ the roots are pure imaginary. The latter satisfies immediately the second geometric constraint (3.78). It is worth meaning that if $\Lambda < 0$, then $-\frac{q^2}{\Lambda} > a^2$. This implies that $\Lambda \neq -\frac{q^2}{a^2}$ is also satisfied, which correspond to the condition to avoid the non-regularity of the curvature scalars for the isotropic and decoupler sector in the limit when $r \to 0$.

In the section 3.1 it was used $\Lambda = 2$ and $\Lambda = -2$. In the first case for $\Lambda = 2$, the second geometrical constrain (3.78) is satisfied and in consequence it is observed a regular behaviour in the curvature scalars [17]. On the other hand, for $\Lambda = -2 < 0$, in the section 3.1 it was found some problems with the regularity. So, let us study the behaviour of the scalars as $r \to \tilde{r}_2 = \pm \sqrt{\frac{-q^2 - a^2 \Lambda}{\Lambda}}$ for $\tilde{r}_2 \in \mathbb{R}$.

For now on, we are going to follow the same procedure as in section 3.3.3 for $r \to \tilde{r}_2$.

Total Sector

Let us consider the line elements for the total sector (3.26) and the solution (**??**) [17] [46]. Then, the total sector scalars are given by,

$$R_{tot} = -f''(r) - \frac{2f'(r)}{r} \tag{3.110}$$

$$\mathcal{R}cc_{tot} = \frac{r^2 f''(r)^2 + 3f'(r)^2 + 2rf'(r)f''(r)}{2r^2} \tag{3.111}$$

$$\mathcal{K} = f''(r)^2 + \frac{2f'(r)^2}{r^2}. \tag{3.112}$$

Notice, that for this case we can skip the geometrical analysis due to the regularity of the total sector do not depend on $f'(r)$.

Isotropic Sector

With resepect to the isotropic sector, we obtain

$$\lim_{r \to \tilde{r}_2} R_{iso} = \text{Indeterminate}, \tag{3.113}$$

$$\lim_{r \to \tilde{r}_2} \mathcal{R}cc_{iso} = \pm\infty, \tag{3.114}$$

$$\lim_{r \to \tilde{r}_2} \mathcal{K}_{iso} = \pm\infty. \tag{3.115}$$

Decoupler Sector

Whereas the decoupler sector scalars read as

$$\lim_{r \to \tilde{r}_2} R_{coup} = \pm\infty, \tag{3.116}$$

$$\lim_{r \to \tilde{r}_2} \mathcal{R}cc_{coup} = \pm\infty, \tag{3.117}$$

$$\lim_{r \to \tilde{r}_2} \mathcal{K}_{coup} = \pm\infty. \tag{3.118}$$

For the isotropic and decoupler sector, all the curvature scalars goes to infinity as $r \to \tilde{r}_2$ violating (3.79). This explain the divergent behaviour found on the section 3.1 for $\Lambda < 0$.

In summary, in this chapter we presented an initial review of a specific black hole solution in (2+1)- dimensions under inverse MGD, to illustrate the duality (Section 3.1). After that, we analyze a general anisotropic (2+1) dimensional model, finding a set of constraints to ensure $\rho > 0$ (3.48)-(3.56) and regularity (3.77)-(3.79) for all the sectors obtained by inverse MGD. Moreover, we showed that BTZ act as an upper bound for the energy constraints (3.48)-(3.49). Finally, we showed that our constraints explain the duality found in the solution used in Section 3.1 from where we conjecture that the apparition of dualities in the implementation of the inverse problem is unavoidable.

Chapter 4

Conclusions & Outlook

We have obtained constraints to the seed anisotropic spherically symmetric solutions of the form (3.26) for three-dimensional gravity used in the inverse MGD program. First, we focused on the non-negativity of the energy density for the three sectors. We found that it is necessary to satisfy four constraints (3.48) - (3.56): two of them correspond to satisfy a differential inequality; one related to the non-vanishing derivative of the function $f(r)$; one constraint to the constant of integration c_1 and the coupling parameter of MGD α. In the same way, it was shown that BTZ black hole solution satisfies the saturated inequality presented in the second constraint (3.49). Moreover, BTZ black hole solution satisfy all the energy constraints if the value of the cosmological constant take values of $\pm \sqrt{-\frac{\alpha c_1}{4}}$. After studying the geometrical part of the sectors, which are related to the regularity of the solutions, it was obtained two weak constraints for $f(r)$, listed in (3.77)-(3.79), to avoid irregular solutions for all the sectors under inverse MGD: one constraint related to the evaluation of the limits of the scalars when the radial parameter goes to zero, and the other one related to the evaluation of the limits when r goes to the roots of $f'(r)$. They were called weak conditions because requires a direct evaluation of the limits of the scalars of curvature and they do not correspond to a more fundamental explanation to the divergent behaviour. Later, we focused to explain the dualities found in section 3.1. Regarding the energy conditions, we found that for the parameter $a = 0.1$, considered in section 3.1, the first constraint (3.48) was immediately violated. Furthermore, it was found that the dependence of the sign of Λ is given by the nature of the roots of the derivative of the function $f(r)$. Even more, it was found that the first (3.48) and second (3.49) constraints were incompatible, for the solution used in the section 3.1 [17][46]. The irregularity problems, found in the review (Section. 3.1), are explained by the second geometrical constraint (3.78), which requires positive values of Λ in order to avoid real roots for $f'(r)$, condition that directly contradicts the energy constraints. The results obtained from the proposed constraints explains the duality behaviour summarized in the table (3.1). Finally, it was shown the relevance of the energy and geometric constraints obtained in this graduation project in the study of dualities under MGD.

However, we suggest that a more rigorous approach to the geometrical constraints is required. We think that the Dimnikova conjecture, related to the De Sitter core for solutions that satisfy the WEC[47], is involved in the regularity of the sources obtained by inverse MGD, because it modifies the core of the seed solution. Finally, we also plan

to focus our attention on the extended inverse MGD method, in which the modification in the time part of the line element is also taken into account.

Appendix A

Construction of Energy-Momentum Tensor: Lagrangian Formulation

The energy momentum tensor could be constructed following the Lagrangian formalism, in which the action for general relativity is given by

$$S = \frac{1}{16\pi} S_H + S_M, \tag{A.1}$$

where S_H corresponds to the Hilbert-Einstein action given by

$$S_H = \int \sqrt{-g} R d^n x. \tag{A.2}$$

where g is the determinant of the metric tensor $g_{\mu\nu}$ and R is the Ricci scalar (2.3).

Now, Let us consider a variation with respect to the metric to (A.1),

$$\delta S = \frac{1}{16\pi} \delta S_H + \delta S_M. \tag{A.3}$$

First, let us consider only the Hilbert-Einstein action for a four dimensional case,

$$\delta_g S_H = \int \delta_g \left(\sqrt{-g} R \right) d^4 x, \tag{A.4}$$

if consider (2.4), then

$$\delta_g S_H = \int \delta_g \left(\sqrt{-g} g^{\mu n u} R_{\mu\nu} \right) d^4 x, \tag{A.5}$$

which is equivalent to,

$$\delta_g S_H = \int \left[\delta_g \left(\sqrt{-g} \right) g^{\mu\nu} R_{\mu\nu} + \delta_g \left(R_{\mu\nu} \right) \sqrt{-g} g^{\mu\nu} + \delta_g (g^{\mu\nu}) R_{\mu\nu} \sqrt{-g} \right] d^4 x. \tag{A.6}$$

let us rewrite (A.6) as the sum of

$$\delta_g(S_1) = \int \delta_g\left(\sqrt{-g}\right) g^{\mu\nu} R_{\mu\nu} d^4 x, \tag{A.7}$$

$$\delta_g(S_2) = \int \delta_g\left(R_{\mu\nu}\right) \sqrt{-g} g^{\mu\nu} d^4 x, \tag{A.8}$$

$$\delta_g(S_3) = \int \delta_g(g^{\mu\nu}) R_{\mu\nu} \sqrt{-g} d^4 x. \tag{A.9}$$

Next, for (A.7), we need the folowin identity. Given a matrix M, then

$$\frac{\delta \det(M)}{\det(M)} = Tr(M^{-1}\delta M), \tag{A.10}$$

this implies that,

$$\delta_g\left(\sqrt{-g}\right) = -\frac{1}{2}\sqrt{-g} g_{\mu\nu}\delta_g g^{\mu\nu}, \tag{A.11}$$

then (A.7) becomes

$$\delta_g(S_1) = \int \left(-\frac{1}{2}g_{\mu\nu}\sqrt{-g}R\right)\delta_g g^{\mu\nu} d^4 x. \tag{A.12}$$

Now, for (A.8) we are going take the variation of the Ricci tensor, that reads

$$\delta R_{\mu\nu} = \nabla_\rho \delta\Gamma^\rho_{\mu\nu} - \nabla_\nu \delta\Gamma^\rho_{\rho\nu}, \tag{A.13}$$

then,

$$\delta_g(S_2) = \int \sqrt{-g} g^{\mu\nu}\left(\nabla_\rho \delta\Gamma^\rho_{\mu\nu} - \nabla_\nu \delta\Gamma^\rho_{\rho\nu}\right) d^4 x, \tag{A.14}$$

this is equivalent to

$$\delta_g(S_2) = \int \sqrt{-g}\nabla_\sigma\left[g^{\mu\nu}\delta\Gamma^\sigma_{\mu\nu} - g^{\mu\sigma}\delta\Gamma^\rho_{\rho\nu}\right] d^4 x, \tag{A.15}$$

which corresponds to an integral with respecto the natural volume element of the covariant divergence of a vector. Using the Stoke's theorem, this is equal to a boundary contribution at infinity, which evaluate as zero[23]. Therefore,

$$\delta_g(S_2) = 0. \tag{A.16}$$

Finally, let us consider the hole expression (A.6),

$$\delta_g S_H = \int \left(-\frac{1}{2}g_{\mu\nu}R + R_{\mu\nu}\right)\sqrt{-g}\delta_g g^{\mu\nu} d^4 x, \tag{A.17}$$

due to we want to obtain $\delta_g S_H = 0$, we obtain,

$$R_{\mu\nu} - \frac{1}{2}g_{\mu\nu}R = 0. \tag{A.18}$$

Now, we are going to consider the variation of the full normalized action obtaining

$$\frac{\delta S}{\sqrt{-g}\delta_g g^{\mu\nu}} = \frac{1}{16\pi}\left(-\frac{1}{2}g_{\mu\nu}R + R_{\mu\nu}\right) + \frac{\delta S_M}{\sqrt{-g}\delta_g g^{\mu\nu}} = 0, \tag{A.19}$$

if we put in the same form of the Einstein's field equations (2.1), it reads

$$\left(-\frac{1}{2}g_{\mu\nu}R + R_{\mu\nu}\right) = -16\pi\frac{1}{\sqrt{-g}}\frac{\delta S_M}{\delta_g g^{\mu\nu}}, \tag{A.20}$$

comparing with the known Einstein's field equations

$$\left(-\frac{1}{2}g_{\mu\nu}R + R_{\mu\nu}\right) = 8\pi T_{\mu\nu}, \tag{A.21}$$

we obtain that the energy-momentum tensor can be written as

$$T_{\mu\nu} = -2\frac{1}{\sqrt{-g}}\frac{\delta S_M}{\delta g^{\mu\nu}}, \tag{A.22}$$

this correspond to the Lagrangian formulation of the energy-momentum tensor.

Bibliography

[1] Einstein, A. Die Grundlage der allgemeinen Relativitätstheorie [AdP 49, 769 (1916)]. *Annalen der Physik* **2005**, *14*, 517–571.

[2] Clemence, G. M. The Relativity Effect in Planetary Motions. *Reviews of Modern Physics* **1947**, *19*, 361–364.

[3] Dyson, F. W.; Eddington, A. S.; Davidson, C. A Determination of the Deflection of Light by the Sun's Gravitational Field, from Observations Made at the Total Eclipse of May 29, 1919. *Philosophical Transactions of the Royal Society A: Mathematical, Physical and Engineering Sciences* **1920**, *220*, 291–333.

[4] Kennefick, D. Testing relativity from the 1919 eclipse—a question of bias. *Physics Today* **2009**, *62*, 37–42.

[5] Holberg, J. B. Sirius B and the Measurement of the Gravitational Redshift. *Journal for the History of Astronomy* **2010**, *41*, 41–64.

[6] Castelvecchi, D.; Witze, A. Einstein's gravitational waves found at last. *Nature* **2016**,

[7] Abbott, B. *et al.* Observation of Gravitational Waves from a Binary Black Hole Merger. *Physical Review Letters* **2016**, *116*.

[8] Delgaty, M.; Lake, K. Physical acceptability of isolated, static, spherically symmetric, perfect fluid solutions of Einstein's equations. *Computer Physics Communications* **1998**, *115*, 395–415.

[9] Lake, K. All static spherically symmetric perfect-fluid solutions of Einstein's equations. *Physical Review D* **2003**, *67*.

[10] Boonserm, P.; Visser, M.; Weinfurtner, S. Generating perfect fluid spheres in general relativity. *Physical Review D* **2005**, *71*.

[11] Lake, K. Galactic Potentials. *Physical Review Letters* **2004**, *92*.

[12] Randall, L.; Sundrum, R. Large Mass Hierarchy from a Small Extra Dimension. *Physical Review Letters* **1999**, *83*, 3370–3373.

[13] Randall, L.; Sundrum, R. An Alternative to Compactification. *Physical Review Letters* **1999**, *83*, 4690–4693.

[14] OVALLE, J. THE SCHWARZSCHILD'S BRANEWORLD SOLUTION. *Modern Physics Letters A* **2010**, *25*, 3323–3334.

[15] OVALLE, J. EFFECTS OF DENSITY GRADIENTS ON BRANEWORLD STARS. 2012; `https://doi.org/10.1142/9789814374552_0447`.

[16] Contreras, E. Minimal Geometric Deformation: the inverse problem. *The European Physical Journal C* **2018**, *78*.

[17] Contreras, E. Gravitational decoupling in 2+1 dimensional space-times with cosmological term. *Classical and Quantum Gravity* **2019**, *36*, 095004.

[18] Contreras, E.; Bargueño, P. Minimal geometric deformation in asymptotically (A-)dS space-times and the isotropic sector for a polytropic black hole. *The European Physical Journal C* **2018**, *78*.

[19] Lee, J. M. *Introduction to Riemannian Manifolds*; Springer International Publishing, 2018.

[20] Wald, R. *General relativity*; University of Chicago Press: Chicago, 1984.

[21] Irgens, F. *Continuum mechanics*; Springer: Berlin, 2008.

[22] Zee, A. *Einstein gravity in a nutshell*; In a nutshell; 2013.

[23] Carroll, S. M. Lecture Notes on General Relativity, arXiv:gr-qc/9712019. 1997.

[24] Schwarzschild, K. On the gravitational field of a mass point according to Einstein's theory. **1999**,

[25] Finkelstein, D. Past-Future Asymmetry of the Gravitational Field of a Point Particle. *Physical Review* **1958**, *110*, 965–967.

[26] EDDINGTON, A. S. A Comparison of Whitehead's and Einstein's Formulæ. *Nature* **1924**, *113*, 192–192.

[27] Christodoulou, D. Examples of Naked Singularity Formation in the Gravitational Collapse of a Scalar Field. *The Annals of Mathematics* **1994**, *140*, 607.

[28] Bañados, M.; Teitelboim, C.; Zanelli, J. Black hole in three-dimensional spacetime. *Physical Review Letters* **1992**, *69*, 1849–1851.

[29] Herrera, L.; Ospino, J.; Prisco, A. D. All static spherically symmetric anisotropic solutions of Einstein's equations. *Physical Review D* **2008**, *77*.

[30] Ovalle, J. Extending the geometric deformation: New black hole solutions. *International Journal of Modern Physics: Conference Series* **2016**, *41*, 1660132.

[31] Casadio, R.; Ovalle, J.; da Rocha, R. The minimal geometric deformation approach extended. *Classical and Quantum Gravity* **2015**, *32*, 215020.

[32] OVALLE, J. SEARCHING EXACT SOLUTIONS FOR COMPACT STARS IN BRANEWORLD: A CON-JECTURE. *Modern Physics Letters A* **2008**, *23*, 3247–3263.

[33] Damour, T. *The twelfth Marcel Grossmann Meeting : on recent developments in theoretical and experimental general relativity, astrophysics and relativistic field theories : proceedings of the MG12 Meeting on General Relativity, UNESCO Headquarters, Paris, France, 12-18 July 2009*; World Scientific: Singapore, 2012.

[34] Ovalle, J.; Gergely, L. Á.; Casadio, R. Brane-world stars with a solid crust and vacuum exterior. *Classical and Quantum Gravity* **2015**, *32*, 045015.

[35] Casadio, R.; Ovalle, J.; da Rocha, R. Classical tests of general relativity: Brane-world Sun from minimal geometric deformation. *EPL (Europhysics Letters)* **2015**, *110*, 40003.

[36] Cavalcanti, R. T.; da Silva, A. G.; da Rocha, R. Strong deflection limit lensing effects in the minimal geometric deformation and Casadio–Fabbri–Mazzacurati solutions. *Classical and Quantum Gravity* **2016**, *33*, 215007.

[37] Mak, M.; Harko, T. Anisotropic stars in general relativity. *Proceedings of the Royal Society of London. Series A: Mathematical, Physical and Engineering Sciences* **2003**, *459*, 393–408.

[38] Chakraborty, B.; Gupta, K. S.; Sen, S. Topology, cosmic strings and quantum dynamics – a case study with graphene. *Journal of Physics: Conference Series* **2013**, *442*, 012017.

[39] Garcia, G. Q.; PorfÃrio, P. J.; Moreira, D. C.; Furtado, C. Graphene wormhole trapped by external magnetic field. 2019.

[40] Witten, E. 2 + 1 dimensional gravity as an exactly soluble system. *Nuclear Physics B* **1988**, *311*, 46–78.

[41] Witten, E. Three-Dimensional Gravity Revisited. 2007.

[42] Achúcarro, A.; Townsend, P. A Chern-Simons action for three-dimensional anti-de Sitter supergravity theories. *Physics Letters B* **1986**, *180*, 89–92.

[43] Gott, J. R.; Alpert, M. General relativity in a (2 + 1)-dimensional space-time. *General Relativity and Gravitation* **1984**, *16*, 243–247.

[44] Contreras, E. Minimal Geometric Deformation: the inverse problem. *The European Physical Journal C* **2018**, *78*, 678.

[45] Contreras, E.; Rincón, Á.; Bargueño, P. A general interior anisotropic solution for a BTZ vacuum in the context of the minimal geometric deformation decoupling approach. *The European Physical Journal C* **2019**, *79*.

[46] He, Y.; Ma, M.-S. (2 + 1)-dimensional regular black holes with nonlinear electrodynamics sources. *Physics Letters B* **2017**, *774*, 229–234.

[47] Dymnikova, I. The cosmological term as a source of mass. *Classical and Quantum Gravity* **2002**, *19*, 725–739.